



POLYHYDROXYALKANOATE PRODUCTION ON REAL FERMENTED WASTEWATER

COMPARISON OF REACTOR MODE AND MECHANISTIC DEFINITION OF STORAGE RESPONSES

CHARLES GAN

Research Supervisors: Dr. Nicolas Derlon, Antoine Brison
EPFL Professors: Dr. Christof Holliger

Abstract

Wastewater resource recovery facilities (WRRFs) equipped with polyhydroxyalkanoate production schemes are the new way forward. These systems function by converting volatile fatty acids derived from fermented waste sludge into PHA and are projected to be more beneficial compared to other WRRF types in terms of value. While promising, currently there are challenges in upscaling the technology and further investigation is needed in finding the best reactor operation mode for real fermented wastewater. Furthermore, more research is needed on determining the mechanisms behind selection of PHA-storers and the storage of PHA thereafter. In this study, a novel aerobic continuously stirred tank reactor (CSTR) is compared with an aerobic sequencing batch reactor (SBR) in parallel. The same, nitrogen limited and fermented, municipal wastewater feed is used for both reactors.

This study was split in two phases, one phase where particulates remained in the influent, and another phase with particulates removed from the influent. The removal of particulates provided more representative characterization of the performance of both reactors by mitigating the underrepresentation of PHA content and the overestimation of PHA yield hypothesized in previous work. Furthermore, selection and storage mechanisms are better visualized with the removal of particulates which provided unintended nutrients through hydrolysis.

Results show that the selection of PHA-storers occurred for both reactors before and after solids removal. This was established by the observation of PHA accumulation during batch tests for both selected biomasses. After solids removal, PHA content reached 21 wt% PHA and 32 wt% PHA for the CSTR and SBR selected biomasses, respectively. These values differed from values measured before solids removal and indicate that influent composition and reactor environmental conditions may play a governing role in PHA storage. General examination of Spearman correlations between influent/reactor conditions and PHA content/composition show that the SBR selected biomass is generally more correlated with reactor loading and the CSTR selected biomass is generally more correlated with influent nutrient availability. While these findings are interesting, specific causation cannot be confirmed in this study without controlled long-term selection monitoring or additional batch testing isolating specific influent and reactor conditions. The practice of isolating a specific influent condition was done in this study. The accumulation batch tests performed in this study addressed nitrogen limitation as a potential governing factor for PHA storage in both reactors. Results suggest that nitrogen limitation does not govern storage within the SBR selected biomass but does for the CSTR selected biomass.

Keywords: polyhydroxyalkanoates (PHA), organic waste, resource recovery, culture selection, nitrogen limitation

Résumé

Les installations de récupération des ressources en eaux usées (WRF) équipées de systèmes de production de polyhydroxyalcanoate sont la nouvelle voie à suivre. Ces systèmes fonctionnent en convertissant les acides gras volatils (AGV) dérivés des boues résiduaire fermentées en PHA et devraient être plus avantageux que les autres types de WRF en termes de valeur. Bien que prometteuse, la mise à l'échelle de cette technologie pose actuellement des problèmes et des recherches supplémentaires sont nécessaires pour trouver le meilleur mode de fonctionnement du réacteur pour les eaux usées fermentées réelles. En outre, des recherches supplémentaires sont nécessaires pour déterminer les mécanismes qui sous-tendent la sélection des stockeurs de PHA et le stockage des PHA par la suite. Dans cette étude, un nouveau réacteur continu (aérobie) (CSTR) est comparé à un réacteur discontinu (aérobie) (SBR) en parallèle. La même eau usée municipale fermentée et limitée en azote est utilisée dans les deux réacteurs.

Cette étude a été divisée en deux phases, une phase où les particules restent dans l'influent, et une autre phase où les particules sont retirées de l'influent. L'élimination des particules a permis une caractérisation plus représentative de la performance des deux réacteurs en atténuant la sous-représentation du contenu en PHA et la surestimation du rendement en PHA supposées dans les travaux précédents. En outre, les mécanismes de sélection et de stockage sont mieux visualisés grâce à l'élimination des particules qui fournissaient des nutriments involontaires par hydrolyse.

Les résultats montrent que la sélection des stockeurs de PHA s'est produite pour les deux réacteurs avant et après l'élimination des matières solides. Ceci a été établi par l'observation de l'accumulation de PHA pendant les tests en lots pour les deux biomasses sélectionnées. Après l'élimination des solides, la teneur en PHA a atteint 21 % en poids de PHA et 32 % en poids de PHA pour les biomasses sélectionnées dans le CSTR et le SBR, respectivement. Ces valeurs différaient des valeurs mesurées avant l'élimination des solides et indiquent que la composition de l'influent et les conditions environnementales du réacteur peuvent jouer un rôle déterminant dans le stockage des PHA. L'examen général des corrélations de Spearman entre les conditions de l'influent/du réacteur et la teneur/composition en PHA montre que la biomasse sélectionnée par le SBR est généralement plus corrélée à la charge du réacteur et que la biomasse sélectionnée par le CSTR est généralement plus corrélée à la disponibilité des nutriments de l'influent. Bien que ces résultats soient intéressants, la causalité spécifique ne peut pas être confirmée dans cette étude sans un suivi contrôlé de la sélection à long terme ou des tests de lots supplémentaires isolant les conditions spécifiques de l'influent et du réacteur. La pratique d'isoler une condition d'influent spécifique a été faite dans cette étude. Les tests d'accumulation par lots effectués dans cette étude ont abordé la limitation de l'azote comme un facteur potentiel régissant le stockage des PHA dans les deux réacteurs. Les résultats suggèrent que la limitation de l'azote ne régit pas le stockage dans la biomasse sélectionnée par le SBR mais le fait pour la biomasse sélectionnée par le CSTR.

Mots-clés: polyhydroxyalcanoates (PHA), déchets organiques, récupération des ressources, sélection des cultures, limitation de l'azote.

Table of Contents

Abstract	<i>i</i>
Résumé	<i>ii</i>
List of Tables	v
List of Figures	vi
1 Introduction	1
1.1 Context	1
1.2 Microbial Storage of PHAs	2
1.3 Engineered application of wastewater PHA production	3
1.3.1 Reactor type on selection: SBR system	4
1.3.2 Reactor type on selection: CSTR system	5
1.3.3 Accumulation reactor to induce maximum storage.....	5
1.3.4 Nitrogen availability effect on reactor performance	5
1.4 Research Gap	6
1.4.1 Research Objectives	7
2 Methodology	8
2.1 Overall experimental setup	8
2.1.1 Fermenter and ultrafiltration membrane operation	8
2.1.2 SBR and CSTR operation	9
2.1.3 Reactor startup and maintenance.....	10
2.1.4 Accumulation batch tests	10
2.2 Sampling and measurement of indicators	11
2.2.1 TS/VS	12
2.2.2 PHA	12
2.2.3 Total and Soluble Compounds	13
2.2.4 VFAs	13
2.3 Calculations	13
2.3.1 Influent calculations	13
2.3.2 Reactor calculations.....	14
3 Results	16
3.1 Influent feed composition	16

3.2 Long-term reactor performance	18
3.2.1 PHA content and composition of reactor biomass.....	19
3.3 Accumulation batch results.....	25
4 Discussion	28
4.1 Effect of removal of solids on PHA content and yield.....	28
4.2 Selection within the reactors: SBR vs. CSTR.....	29
4.3 Link between influent composition, selection of storing organisms, and PHA storage	30
4.3.1 Spearman correlation matrix: PHA content	30
4.3.2 Accumulation batch test: PHA content	31
4.3.3 Spearman correlation matrix: PHA composition	32
4.3.4 Accumulation batch test: PHA composition	32
5 Conclusion.....	33
References	34
Appendix	36
<i>Appendix A: Batch 5a (a), 5b (b), 6a (c), and 6b (d) results showing PHA accumulation, consumption of sCOD and increase of pCOD over length of batch. Batches were stopped when sCOD consumption plateaued.</i>	<i>36</i>

List of Tables

TABLE 1: THEORETICAL CONDITIONS FOR THE BATCH TESTS PERFORMED. BATCH 5 AND 6 ARE COMPLETED WITHIN A ONE-WEEK TIME SPAN. SUB-BATCH 5A AND 5B WERE CONDUCTED SIMULTANEOUSLY IN TANDEM TO COMPARE THE EFFECT OF NITROGEN AVAILABILITY ON ACCUMULATION IN THE SBR SELECTED BIOMASS. SUB-BATCH 6A AND 6B WERE ALSO CONDUCTED IN PARALLEL TO COMPARE THE EFFECT OF NITROGEN AVAILABILITY IN THE CSTR SELECTED BIOMASS.	11
TABLE 2: INFLUENT COMPOSITION IN TERMS OF CONCENTRATION AND PERCENTAGE OF TOTAL VFA BEFORE AND AFTER THE REMOVAL OF SOLIDS BY ULTRAFILTRATION.	17
TABLE 3: REACTOR TREATMENT CAPABILITIES REPRESENTED BY LOW EFFLUENT CONCENTRATION OF NUTRIENTS AND HIGH REMOVAL EFFICIENCY. EFFLUENT REFERS TO THE SAMPLES TAKEN DURING THE DECANT OR END OF FAMINE PHASE FOR THE SBR AND REFERS TO THE CONTINUOUS OUTFLOW FOR THE CSTR.	19
TABLE 4: SBR AND CSTR PHA CONTENT BY SPECIES TYPE AND THE RATIO BETWEEN P(3HB) AND P(3HV) BEFORE AND AFTER SOLIDS REMOVAL.	21

List of Figures

FIGURE 1: A PROCESS SCHEME THAT IS COMMONLY USED FOR PHA PRODUCTION INTEGRATION IN MUNICIPAL WASTEWATER TREATMENT PLANTS. PHAS REPRESENTS A LARGE GROUP OF POLYESTERS WHICH CAN BE REFINED TO PRODUCE USABLE BIOPLASTIC.	2
FIGURE 2: METABOLIC PATHWAY FOR PRODUCTION OF VFAs AND SYNTHESIS OF INTRACELLULAR GRANULAR PHAS (REIS ET AL., 2011; SZACHERSKA ET AL., 2021).	2
FIGURE 3: REPRESENTATION OF FEAST AND FAMINE PHASE IN AN SBR WHERE CARBON SUBSTRATES (VFAs) ARE AVAILABLE AT THE BEGINNING AND NOT IN THE END, IN TURN FAVORING ORGANISMS WITH PHA STORE IN THE FAMINE PHASE (ADAPTED FROM REIS ET AL., 2011). THE RED LINE REPRESENTS THE SPECIFIC GROWTH RATE OF THE MICROORGANISM, THE BLUE LINE REPRESENTS THE VFA CONCENTRATION, AND THE GREEN LINE REPRESENTS THE PHA CONCENTRATION.	4
FIGURE 4: DETAILED EXPERIMENTAL SETUP FOR LONG-TERM SELECTION MONITORING AND SHORT-TERM ACCUMULATION BATCH TESTS (ADAPTED FROM BETTEX, 2021). THIS SETUP INCLUDES AN ADDITIONAL ULTRAFILTRATION MEMBRANE WHICH REMOVES INCOMING PARTICULATES.	8
FIGURE 5: IDENTIFICATION OF END OF FEAST PHASE FOR THE SBR SELECTION REACTOR. BLACK LINE REPRESENTS CHANGING OXYGEN LEVELS IN THE REACTOR FROM 2.5 TO 3.0 MG AND GREEN LINE REPRESENTS CHANGING PH IN THE REACTOR TYPICALLY FROM 8.5 TO 9.5. GREEN SHADED AREA REPRESENTS THE INITIAL FILL PHASE OF EACH SBR CYCLE WHERE PH DROPS, AND HIGH OXYGEN CONSUMPTION BEGINS. RED SHADED AREA REPRESENTS THE FEAST PHASE WHERE ACIDS ARE CONSUMED AND PH INCREASES. GREY SHADED AREA REPRESENTS FAMINE PHASE WHERE VFAs ARE DEPLETED. YELLOW SHADED AREA REPRESENTS DECANT PHASE WHERE BIOMASS IS WASTED BEFORE THE NEXT CYCLE FILL.	10
FIGURE 6: EVOLUTION OF INFLUENT COMPOSITION BEFORE AND AFTER SOLIDS REMOVAL (RED BOX): INFEED IS DOMINATED BY PROPIONATE BEFORE AND AFTER SOLIDS REMOVAL. THE KEY DIFFERENCE AFTER SOLIDS REMOVAL IS THE DECREASED PRESENCE OF PCOD.	17
FIGURE 7: INFLUENT NITROGEN AND PHOSPHOROUS NUTRIENT AVAILABILITY BEFORE AND AFTER SOLIDS REMOVAL.	18
FIGURE 8: SBR PHA CONTENT AT THE END OF FEAST PHASE REPRESENTED BY BLUE BARS FOR P(3HB) AND RED BARS FOR P(3HV), THE RED BOX INDICATES THE TIME PERIOD AFTER THE REMOVAL OF SOLIDS FROM THE INFLUENT AND THE BLACK CIRCLES REPRESENT THE TOTAL PHA MEASURED AT THE END OF CYCLE OR FAMINE PHASE.	19
FIGURE 9: CSTR PHA CONTENT WITH BLUE BARS REPRESENTING P(3HB) AND RED BARS REPRESENTING P(3HV), THE RED BOX INDICATES THE TIME PERIOD AFTER THE REMOVAL OF SOLIDS FROM THE INFLUENT.	20
FIGURE 10: AVERAGE SBR AND AVERAGE CSTR PHA CONTENT SEPARATED BY PHA SPECIES BEFORE AND AFTER SOLIDS REMOVAL. BARS ARE OFFSET TO AVOID OVERLAPPING ERROR BARS. FOR THE SBR, THE TWO AVERAGE VALUES ARE NOT SIGNIFICANTLY DIFFERENT (P-VALUE = 0.26). HOWEVER, THE CSTR AVERAGES ARE SIGNIFICANTLY DIFFERENT (P-VALUE = 0.01) WITH A 240% INCREASE AFTER SOLIDS REMOVAL.	20
FIGURE 11: AVERAGE SBR AND CSTR PHA YIELD BEFORE AND AFTER SOLIDS REMOVAL. FOR THE SBR, THE TWO AVERAGE VALUES ARE NOT SIGNIFICANTLY DIFFERENT (P-VALUE = 0.43). HOWEVER, THE CSTR AVERAGES ARE SIGNIFICANTLY DIFFERENT (P-VALUE = 9E-9) WITH A 74% DECREASE AFTER SOLIDS REMOVAL.	21
FIGURE 12: SBR (A) AND CSTR (B) CORRELATION MATRIX SHOWING THE SPEARMAN CORRELATION BETWEEN INFLUENT/REACTOR PARAMETERS AND PHA CONTENT/COMPOSITION. DARKER GREEN SHADED BOXES	

INDICATE INCREASING POSITIVE CORRELATION, DARKER RED SHADED BOXES INDICATE INCREASING NEGATIVE CORRELATION, AND WHITE BOXES INDICATE NO CORRELATION. STARS INDICATE P-VALUE SIGNIFICANCE WITH * MEANING P-VALUE < 0.05, ** FOR P-VALUE < 0.01, AND *** FOR P-VALUE < 0.001.24

FIGURE 13: SBR PHA CONTENT AND COMPOSITION AT THE START AND AT THE MAXIMUM VALUE OF ACCUMULATION BATCHES (PHB IS P(3HB), PHV IS P(3HV)).26

FIGURE 14: CSTR PHA CONTENT AND COMPOSITION AT THE START AND AT THE MAXIMUM VALUE OF ACCUMULATION BATCHES (PHB IS P(3HB), PHV IS P(3HV)).26

FIGURE 15: SBR PHA YIELD THE SAMPLING DAY BEFORE AND ON THE DAY OF THE ACCUMULATION BATCH.27

FIGURE 16: CSTR PHA YIELD THE SAMPLING DAY BEFORE AND ON THE DAY OF THE ACCUMULATION BATCH.27

FIGURE 17: SBR (A) AND CSTR (B) RELATIVE PHA INCREASE PERCENTAGE DURING ACCUMULATION BATCHES AS A FUNCTION OF INITIAL NITROGEN AVAILABILITY. TWO POINTS OUTSIDE OF THE 95% CONFIDENCE INTERVAL ARE EXCLUDED FOR THE CSTR.....28

1 Introduction

1.1 Context

Municipal wastewater has long been considered a burdensome byproduct of human activity, imposing costs while providing little value to society. This mindset has changed in recent decades as concerns surrounding climate change have increasingly driven a search for new and alternative sustainable resources. The idea of a circular economy where end products such as wastewater are repurposed and reused has emerged as a promising path forward. Within wastewater, there is an abundance of organic carbon. This has slowly been introduced as a flexible, reusable feed input that can provide value through many resource recovery operations such as biofuel production, fertilizer generation, and high-value biopolymer production (Puyol et al., 2017). The latter is a recent development and is especially promising because these biopolymer outputs have been shown to be more cost effective and valuable when compared to biofuel and other recovery value chains (Conca et al., 2020). In a recent study, estimates indicated that the production of bioplastics as a side stream could generate up to 6.5 euros per person equivalent as opposed to only 0.54-0.58 euros per person equivalent for biogas production on its own (Conca et al., 2020). With the rapid decrease in costs and the newly realized opportunity to valorize a global waste stream, the exploration of easier and more innovative process schemes is becoming an attractive area of research that could further encourage widespread market adoption.

The recent research on biopolymer production focuses on using specialized wastewater bacteria to convert organic carbon to biopolymers called PolyHydroxyAlkanoates (PHAs – bioplastic precursors). Normally, this requires a process scheme with three primary steps: first the capture of organic carbon, then anaerobic fermentation, and finally the selection and accumulation of PHA for end product extraction (Figure 1). The capture of organic carbon is well understood and usually consists of taking settled solids during primary clarification or secondary clarification. Anaerobic fermentation is also understood, its main function is to convert organic carbon in solid particulate form into a soluble carbon substrate in which microorganisms can more easily uptake and convert. The most pressing challenges in the optimization of PHA production come from the definition of the last step. There are many unique feedstocks globally and to be able to understand how to apply the best system for each context, first a detailed understanding of microorganism behavior must be established and then an engineering scheme must be designed to take advantage of this behavior.

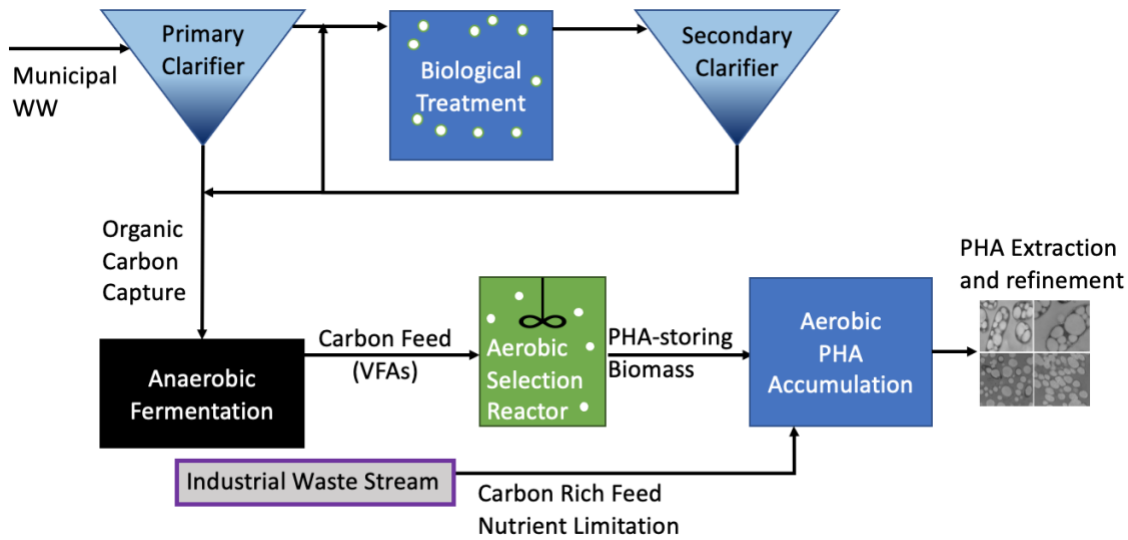


Figure 1: A process scheme that is commonly used for PHA production integration in municipal wastewater treatment plants. PHAs represents a large group of polyesters which can be refined to produce usable bioplastic.

1.2 Microbial Storage of PHAs

PHA synthesis is a behavior associated with over 300 bacterial species present in wastewater (Coats et al., 2007). The purpose of biopolymers being formed by these microorganisms is twofold: (i) to store carbon substrate for later use and (ii) to use as an electron donor for energy. When speaking of PHA production, the former is the mechanism of interest. When specific microbial communities are placed in excess carbon environments under growth-limited conditions (i.e. a lack of nitrogen, phosphorous, magnesium, oxygen, etc.), storing carbon-based polymers becomes advantageous for continued propagation and survival (Dionisi et al., 2004). Within the wastewater context, the preferred carbon substrates for microorganism consumption are Volatile Fatty Acids (VFAs) which are readily biodegradable and direct precursors for PHA formation. These organic acids can be dosed to induce the previously stated conditions which incentivize storage (Valentino et al., 2017).

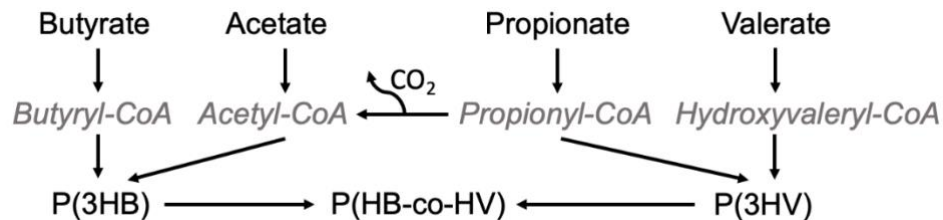


Figure 2: Metabolic pathway for production of VFAs and synthesis of intracellular granular PHAs (Reis et al., 2011; Szacherska et al., 2021).

The dosing of different VFAs can induce the production of varied PHA compounds (Figure 2). Therefore, understanding the main pathways for converting VFAs to PHAs is important for

understanding which PHAs will be produced. Microorganisms can readily process and uptake VFAs using Coenzyme A (CoA), which is naturally present in fermented wastewater. This enzyme is a key component in the biosynthesis pathway and, paired with VFAs, functions directly as a precursor for basic metabolic functions (Szacherska et al., 2021). CoA functions differently depending on the fatty acid present and generates a range of derivatives such as (R)-3-hydroxyvaleryl-CoA, acetyl-CoA, butyryl-CoA, and propionyl-CoA. These derivatives have different properties in that some can only oxidate odd-chain fatty acids (propionyl-CoA and (R)-3-hydroxyvaleryl-CoA) while others are able to oxidate even-chain fatty acids (acetyl-CoA, butyryl-CoA). While CoA derivatives are generally set in their pathways to PHA-species, some can be transformed. For example, propionyl-CoA can be decarboxylated to acetyl-CoA. Consequently then, knowledge of the initial presence of coenzyme derivatives or fatty acid composition isn't necessarily enough to predict the final PHA-species composition.

Although it is not possible to quantify specific composition, knowing the presence of specific fatty acids and CoA derivatives can give some indications of what to expect in terms of biopolymer type that will be later extracted for market use. For example, the presence of propionate under certain conditions can favor polyhydroxyvalerate P(3HV) over polyhydroxybutyrate P(3HB) while the presence of acetate can only form P(3HB). This distinction is important because the ratio of P(3HV) to P(3HB) creates plastic with different market applications due to their differing thermoelastic properties. High P(3HB) to P(3HV) ratio, for example, creates a brittle and stiff material while low P(3HV) to P(3HB) ratio is more flexible (Kourmentza et al., 2017).

1.3 Engineered application of wastewater PHA production

With the understanding of how microorganisms use VFAs to create different types PHAs, the next important step is to take advantage of this mechanism in an engineered wastewater system. Previous studies have already verified the possibility of PHA production using refined, high carbon substrate wastewater and pure cultures of PHA-storing bacteria (Braunegg et al., 1998). However, this method is costly and requires specialized conditions to keep the pure culture isolated and wastewater sterile (Coats et al., 2007). In recent decades, research has shifted towards the use of mixed microbial cultures (MMCs) and real fermented wastewater feeds. This allows for the possibility of retrofitting existing wastewater treatment plants, which significantly reduces operational costs and paves the path for the scaling of PHA production for industry use.

Currently, typical setups for producing PHA using wastewater MMCs follow a multi-step approach:

- i) a wastewater feed is processed to capture organic carbon,
- ii) the carbon is converted into VFAs (the building blocks of biopolymers) using anaerobic fermentation,
- iii) the VFA feed is supplied to a *selection* reactor where PHA storing bacteria are selected from MMCs as a result of internal reactor conditions (nutrient availability, transient carbon, influent composition, etc.),
- iv) PHA is accumulated in another subsequent *accumulation* reactor to maximize PHA content and finally,
- v) PHA is extracted and refined for sale in the market.

Steps (iii), (iv) and (v) are the current area of interest for expanding PHA production to more wastewater systems.

1.3.1 Reactor type on selection: SBR system

One potential type of selection reactor that is currently state-of-the-art is the Sequencing Batch Reactor (SBR). The SBR selects a consortium of PHA-storing bacteria by implementing alternating phases of high substrate availability (feast phase) and low substrate availability (famine phase) (Figure 3). During the famine phase, bacteria that store carbon have a competitive advantage over those that do not store and are able to grow on stored carbon. Those that do not store at high rates starve and are unable to live on to the next cycle. Over multiple cycles, an SBR is therefore able to select for PHA-storing bacteria which can then be used for PHA accumulation. This type of system is known as a *dynamic feeding system* because the nutrient concentration is transient and changing over time.

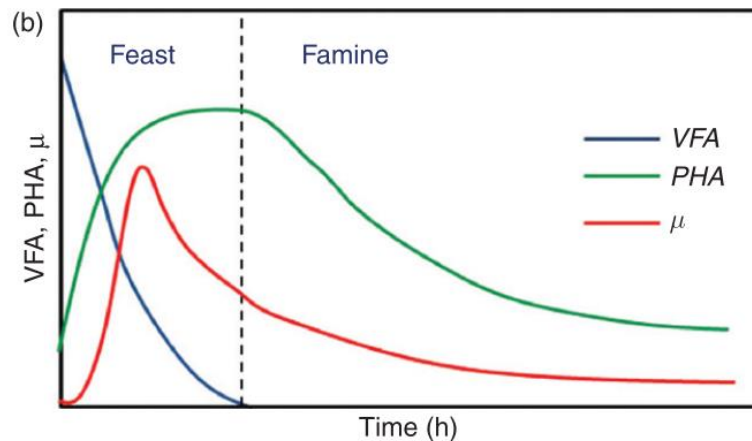


Figure 3: Representation of feast and famine phase in an SBR where carbon substrates (VFAs) are available at the beginning and not in the end, in turn favoring organisms with PHA store in the famine phase (adapted from Reis et al., 2011). The red line represents the specific growth rate of the microorganism, the blue line represents the VFA concentration, and the green line represents the PHA concentration.

While SBRs are effective as selection reactors, they have one key shortfall that leads to poor selection of PHA storers. Using dynamic feeding systems for selection requires there to be low growth limitations and sufficient carbon substrate during the feast phase to allow the selected microorganisms from the previous cycle to propagate. Therefore, feedstocks with growth limitation or substrate limitation are not desirable for SBR implementation and have been shown to actively inhibit the selection process (Albuquerque et al., 2010; Cavaillé et al., 2016). Furthermore, this requirement is counterproductive because, for the following accumulation step, growth limitation

is often found to be beneficial. Therefore, it would be desirable if a selection reactor could be implemented in a way that accommodates growth limitation in the infeed.

1.3.2 Reactor type on selection: CSTR system

Using a Continuous Stirred Tank Reactor (CSTR) as a selection mechanism could provide a novel solution accommodating a wider set of influent types including growth-limiting and high carbon substrate feedstocks. This approach has been shown to work for the selection of PHA-storers when a dual carbon and phosphorous nutrient limitation is imposed (Cavaillé et al., 2016). CSTR reactor systems function by dosing small amounts of infeed and wasting equal amounts continuously over time. This maintains a system where the available nutrients are always limited regardless of the loading of the influent. While the exact mechanism for selection of PHA storers is unknown, it is theorized that selection occurs due to the increased affinity of PHA storers to nitrogen and phosphorous sources, which allows for a competitive edge over the already limited amounts of nutrients being supplied (Johnson et al., 2009). Another theory is that the continuous supply of low doses of carbon favors organisms that have high substrate uptake rates which is a mechanism often linked to the ability to accumulate PHA substrate (Johnson et al., 2009). These collective selective pressures allow the CSTR to function as a more easily implemented selection reactor that can accommodate nutrient limited feedstocks. This is valuable because it is a process scheme that can fit in a larger range of WasteWater Treatment Plants (WWTPs), and it can be more easily integrated with the desired conditions of the accumulation reactor immediately downstream.

1.3.3 Accumulation reactor to induce maximum storage

The purpose of an accumulation reactor is to take the selected PHA-storing biomass from the selection reactor and to feed it excess amounts of carbon substrate under growth limiting conditions to induce maximum storage of PHAs. This process increases the efficiency and the yield of PHAs from the initial source feed. The mechanisms behind what drive this maximum storage are not necessarily the same as the selection mechanisms. Furthermore, the mechanism is also not necessarily the same between the SBR and CSTR selected biomasses. For the SBR biomass, max PHA storage in the subsequent accumulation reactor has been found to occur due to abundant initial carbon substrate, a carbon gradient, and a nutrient limitation to minimize growth (Rhu et al., 2003). This contrasts from the selection stage of the SBR biomass where growth nutrients are beneficial for better selection as mentioned previously. For the CSTR biomass, optimal conditions for max PHA storage are not yet known. However, it is hypothesized that the limitation of nitrogen may be a possible trigger for maximum PHA storage.

1.3.4 Nitrogen availability effect on reactor performance

Nitrogen nutrient presence can have a multifaceted impact on accumulation by increasing PHA species diversity in excess and promoting higher storage in limitation. In a recent study using soil derived MMCs, the presence of excess nitrogen was attributed to increase in growth and heterogeneous microbial communities within wastewater reactors for PHA production (Ntaikou et al., 2019). Furthermore, it was found that heterogeneity in a microbial community resulted in more

varied PHA species composition, which can be detrimental in cases where consistency is desired in the end PHA product (Ntaikou et al., 2019). Nitrogen availability was also tested with activated sludge biomass and brewery wastewater feed with mostly acetate and it was found that a C:N ratio of 125 g_C/g_N is best suited for the maximum PHA content of 59% cell dry weight (Wen et al., 2010). In another study, a C:N ratio of 96 was found to be the best for a yield of 0.11 g_{PHA} per g_{COD} consumed (Ma et al., 2000). From these results, it is suggested that a low nitrogen availability is best for an accumulation reactor with SBR selected biomass.

Although nitrogen availability is important, it has recently been shown to be a secondary constraint to phosphorous availability when using Xylose as an influent feed (Oliveira-Filho et al., 2020). As a primary finding, phosphorous availability was shown to govern the amount of PHA stored and to be a larger determining factor than nitrogen availability. However, microorganisms take longer to adapt to low phosphorous than low nitrogen, indicating that there are multiple dimensions to consider with trying to achieve high PHA yield (Oliveira-Filho et al., 2020). These studies have all been investigated using SBR feeding systems. There has yet to be a study investigating the effect of nitrogen availability on accumulation reactors using CSTR selected biomass.

1.4 Research Gap

Pilot scale operations have been attempted and have succeeded in producing PHA's using real fermented wastewater, MMCs, and an SBR selection reactor followed by an accumulation reactor. Valentino et al. recently showed the successful implementation of PHA production process using fermented municipal wastewater sludge combined with fermented food waste sludge (Valentino et al., 2019). Further, Conca et al. showed the feasibility of side stream PHA production using a pilot scale operation on fermented municipal wastewater (Conca et al., 2020). In total, there have been 19 pilot scale studies conducted successfully using a variety of wastewater feeds and reactor operation modes (Estévez-Alonso et al., 2021). However, this process still needs additional replication with real wastewater to verify widespread applicability and further setups need to be explored to optimize PHA output and the type of PHA produced. Additionally, it is critically important to further investigate the mechanisms behind microorganism storage response in accumulation reactors to better understand how best to maximize PHA production using municipal wastewater. Increased understanding could allow WWTPs that implement this technology to have a better ability to foster suitable conditions for the synthesis of valuable bioplastics. Due to these shortcomings in understanding, a clear demonstration of commercial manufacturing of PHAs from wastewater feed has yet to be achieved, and there are still concerns on how to create market demand and produce a stable supply with desirable thermoelastic properties (Estévez-Alonso et al., 2021).

CSTRs can theoretically be more easily implemented and could be the answer to increasing market supply. This is because the implementation does not require cycle time optimization and it is more adaptable to changing influent loading conditions. As mentioned before, Cavallé et al. demonstrated the possibility to use CSTR under dual carbon and phosphorous limitation to successfully produce PHA at the laboratory scale with *synthetic* influent (Cavallé et al., 2016). However, few studies have been conducted comparing the effectiveness of SBR and CSTR in selecting storing organisms using municipal wastewater-derived feed. Previous research at the

Swiss Federal Research Institute of Aquatic Sciences (Eawag) showed that, although equally viable for the selection of PHA-storers and the accumulation of PHA, the CSTR produced lower PHA content and yield when compared to the SBR (Bettex, 2021). These findings provide initial optimism for the CSTR as a viable method for the selection of PHA storers, but there remain several unanswered questions. In the previous research efforts at Eawag, large particulates remained after acidogenic fermentation and secondary clarification which were then included in the infeed to the PHA selection reactors (Bettex, 2021). This had three potential consequences on the evaluation of both reactor modes tested: (i) influent particulates contain ordinary heterotrophic organisms that compete with the desired PHA storer community, (ii) influent particulates dilute PHA content values (described as $g_{\text{PHA,COD}}$ per g_{pCOD}) by including both non-storers and storers within the g_{pCOD} quantity, and iii) influent particles are hydrolyzed and provide additional nutrients in the form of soluble N/P to the reactors which inadvertently increases nutrient availability and distorts the ability to analyze the connection between incoming soluble nutrient loading with PHA content and yield. Therefore, the current research needs that will be addressed in this study are the evaluation of SBR versus CSTR without particulates.

1.4.1 Research Objectives

The goal of this study is to continue the efforts of the previous research at Eawag in the comparison of a CSTR and an SBR system in parallel for PHA production and to answer two main research questions:

- 1. How does the use of a novel CSTR system affect the selection of PHA-storing organisms (and consequently the PHA storage) when compared to the traditional SBR approach before and after solids removal?**
- 2. To what extent does nitrogen limitation govern the PHA-storage in the different biomasses (CSTR vs. SBR) during accumulation batches?**

2 Methodology

2.1 Overall experimental setup

This thesis was conducted at Eawag located in Dübendorf, Switzerland. The experiment was run for 202 days and had two phases: before solids removal by ultrafiltration (Day 2-146) and after solids removal (Day 146-202). The first phase before solids removal was conducted previously at Eawag by another student (Bettex, 2021). The overall system is composed of three distinct components (Figure 4): (i) a pilot-scale anaerobic digester system that ferments real municipal wastewater from the City of Dübendorf to produce a VFA-rich stream (ii) two laboratory-scale reactors running in parallel comparing two operation modes for selection: SBR and CSTR and (iii) separate periodic accumulation reactor batch tests to assess maximum PHA production in the selected biomass.

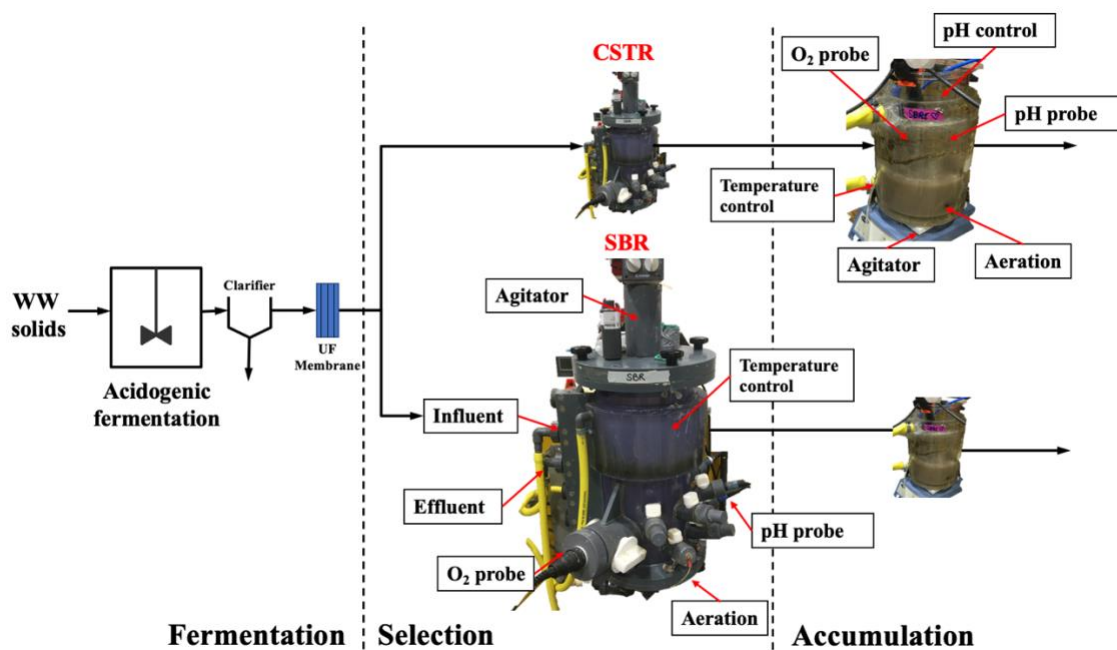


Figure 4: Detailed experimental setup for long-term selection monitoring and short-term accumulation batch tests (adapted from Bettex, 2021). This setup includes an additional ultrafiltration membrane which removes incoming particulates.

2.1.1 Fermenter and ultrafiltration membrane operation

Primary sludge from Eawag WWTP was fermented in a 450-liter pilot-scale anaerobic reactor to produce a VFA-rich feedstock for the selection reactors. The anaerobic digester was fed four times per day at a rate to maintain a steady Solids Retention Time (SRT) of 6.4 days (70 liters per day, 17.5 liters per feed). SRT was maintained at this specific length to inhibit the growth of slow-growing methanogens. Additionally, this SRT was identified in previous studies as preferable for maximum hydrolysis and fermentation of solids to VFAs without methanogenesis (Vanwonterghem et al., 2015). Further, the digester was constantly stirred and kept at 37°C to

induce mesophilic conditions, increase microbiological activity, and concentrate the amount of VFAs produced. After digestion, the VFA rich stream was taken to a secondary clarifier that helped partially remove unwanted solids. Then, the clarified effluent of the secondary clarifier was sent to a separate 100-liter tank with a submerged flat ultrafiltration membrane with a pore size of 150 kDa and a total surface area of 3.5 m² distributed across 9 double sided flat sheet modules. The membrane was incrementally optimized to run six cycles per day for two hours at an average of 1.3 Liters per Meter² per Hour (LMH) resulting in a total volume of around 55 liters. After each cycle, a resting time of two hours occurred and every two cycles there was a 15-minute backwash cycle. The membrane was backwashed with already filtered permeate to avoid dilution of the VFA rich stream.

2.1.2 SBR and CSTR operation

After the membrane, the permeate was pumped up to a 15-liter reserve tank with plastic surface orbs to inhibit oxygen diffusion. Both selection reactors (SBR and CSTR) directly took feed from this permeate tank. This permeate will be from hereafter referred to as “influent”.

Two 12-liter selection reactors were operated in parallel as an SBR and as a CSTR. Both decanted and filled at a rate equivalent to a Solids Retention Time (SRT) and a Hydraulic Retention Time (HRT) of one day (12 liters of influent exchanged for each reactor per day). This SRT and HRT was selected to provide strong selective pressure for organisms with high uptake. High uptake rate is beneficial for the nutrient removal required for wastewater treatment processing as well as the substrate-to-PHA conversion yield.

The main difference between the two reactor modes is the influent feeding regime determined by the inflow and outflow volume control. The SBR was programmed to have six cycles per day consisting of a five-minute fill, four-hour react, and five-minute decant phase. One sixth of the reactor volume (approximately two liters) was removed and filled each cycle to maintain one day SRT. The SBR implemented did not have a settling phase to ensure an HRT equal to SRT, furthering the incentive for high uptake. For the CSTR, the reactor was programmed to fill for six seconds every 234 seconds and to decant one second every 59 seconds at a rate of 8.3 mL/s to maintain an SRT and HRT of one day.

To keep consistent conditions, each reactor was equipped with continuous mixing, Dissolved Oxygen (DO) monitoring, aeration control, pH monitoring, temperature control, and volume control (Figure 4). For both the SBR and the CSTR, reactor control and monitoring were programmed using a logic control system (Citect SCADA, UK). For both reactors, oxygen levels were kept consistently between 2.5 and 3.0 mg/L O₂ using compressed air to ensure aerobic conditions in both reactors. Temperature was controlled at 25°C for both reactors using a thermostatic jacket to keep consistent conditions throughout the long-term experiment. pH was monitored to determine the end of feast phase time for the SBR (Figure 5). The feast phase end point was set at the highest peak pH value and is the point at which PHA content is usually at its maximum (Figure 3). As VFA's are consumed during the feast phase, pH increases and DO decreases with the removal of acids and the increase in microbiological uptake and activity. Then at the end of feast, the pH apexes and begins declining with DO increasing with less microbial activity. The end of feast is important to measure because it is theoretically the point in which storage is highest in

the selected microbial population. Comparing the storage between the end of feast and end of famine can also be a useful insight for determining how well the selection for storers has occurred.

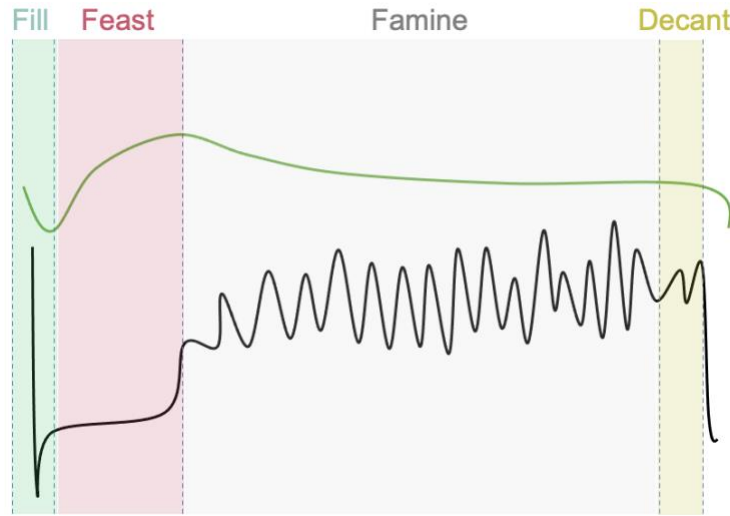


Figure 5: Identification of end of feast phase for the SBR selection reactor. Black line represents changing oxygen levels in the reactor from 2.5 to 3.0 mg and green line represents changing pH in the reactor typically from 8.5 to 9.5. Green shaded area represents the initial fill phase of each SBR cycle where pH drops, and high oxygen consumption begins. Red shaded area represents the feast phase where acids are consumed and pH increases. Grey shaded area represents famine phase where VFAs are depleted. Yellow shaded area represents decant phase where biomass is wasted before the next cycle fill.

2.1.3 Reactor startup and maintenance

Both reactors were initially inoculated with 8 mL of activated sludge from a previous High-Rate Activated Sludge (HRAS) process scheme. Additionally, both reactors were emptied and scoured twice a week with a high-pressure hose to remove biofilm growing on the reactor sides and monitoring probes. Biofilms inhibit the selective pressure of low SRT/HRT, nutrient limitation, and transient carbon gradient by allowing microorganisms to persist on the walls of the reactor from cycle to cycle. It is important to note that this practice of scouring is not common on the pilot scale; the area of biofilm developed in small lab scale reactors are disproportionate in terms of surface area to reactor volume ratio when compared to pilot scale reactors. After scouring, the reactor volume is returned to the reactors and the system is resumed.

2.1.4 Accumulation batch tests

Accumulation reactor batch tests are useful for determining the maximum PHA storage possible for the selected biomass. Two comparison batch tests were completed to better understand the mechanisms behind what induces maximal storage within the selected biomasses in both reactors. The two batch tests were completed within the timespan of one week to reduce the impact of changing influent conditions on the batch results. The main objective for conducting these batch tests was to characterize maximum storage in an accumulation reactor and to

observe the effect of nitrogen availability on PHA storage capacity. For each comparison batch, two five-liter reactors were used, and conditions were established to be similar to the long-term reactors to reduce shock to the biomass. Temperature was set to 25°C with a thermostatic jacket, pH was controlled to match what was typically observed in the long-term reactors the sampling day before (8.3-8.7 for CSTR, 8.5-9.5 for SBR), dissolved oxygen was controlled to 2.5 to 3.0 mg/L O₂, and the reactor was continuously stirred using a magnetic stir bar at the lowest speed setting of 200 rpm. For each comparison batch, one reactor's biomass was used, and two conditions were compared (sub-batch) (Table 1).

Table 1: Theoretical conditions for the batch tests performed. Batch 5 and 6 are completed within a one-week time span. Sub-batch 5a and 5b were conducted simultaneously in tandem to compare the effect of nitrogen availability on accumulation in the SBR selected biomass. Sub-batch 6a and 6b were also conducted in parallel to compare the effect of nitrogen availability in the CSTR selected biomass.

Batch ID	Reactor	Initial VFA Load [mg_{COD}/L]	Composition	COD:N Ratio in Feed	COD:P Ratio in Feed
5a	SBR	1800	100% Propionate	20	100
5b	SBR	1800	100% Propionate	No N added	100
6a	CSTR	1800	100% Propionate	20	100
6b	CSTR	1800	100% Propionate	No N added	100

To try and achieve maximum storage and ensure that there is excess carbon substrate, each five-liter accumulation reactor sub-batch was first filled with one liter of synthetic influent containing VFA's composed of acids typically observed in influent (100% propionate) at four times the typical loading on the reactors. The influent was adjusted with NH₄-N (32%) to have a COD:N ratio of 20 g_{COD}/g_N in one reactor and none was added in the other to maintain a ratio of at least 1000 g_{COD}/g_N to compare the effect of nitrogen availability on storage capacity. Then, KH₂PO₄ was added in both reactors to reach a COD:P ratio of at most 200 g_{COD}/g_P to have phosphorous excess throughout the batch test. The one liter of synthetic influent is warmed to 25°C within each sub-batch reactor and the pH is adjusted with NaOH or HCl to match the long-term reactor pH value to keep constant temperature and pH conditions for the biomass. Four liters of biomass was then extracted from the reactor of interest (two liters per sub-batch). For the SBR, biomass was extracted at the end of the cycle after the famine phase. For the CSTR, no particular condition was required before extraction. The batch test started immediately once the biomass (two liters per batch) was added to the synthetic influent and the first sample was taken. 100mL samples were taken every two hours using a syringe and immediately processed. pH and temperature were also recorded at each sample point to ensure consistent conditions were being observed in the reactors. The batch tests were run until sCOD consumption stopped or was very low.

2.2 Sampling and measurement of indicators

Long-term sampling consisted of taking measurements two times per week every three to four days. 200mL of sample was taken from the top of each reactor at the end of the feast and end of

famine phase for the SBR and taken at a single non-distinct time for the CSTR. 200mL of sample was also taken from the influent permeate container to measure the composition going into each reactor. Samples for the CSTR and influent into the reactors were taken at the same time as the SBR for consistency. For both long-term selection reactors and batch tests Total Solids (TS), Volatile Solids (VS), PHA, ammonium as nitrogen (NH₄-N), phosphate as phosphorous (PO₄-P), Total Chemical Oxygen Demand (TCOD), Soluble Chemical Oxygen Demand (sCOD), and particulate Chemical Oxygen Demand (pCOD) were measured in the reactors. The influent is sampled for VFA's, TCOD, sCOD, pCOD, Total Nitrogen (TN), Total Phosphorous (TP), PO₄-P and NH₄-N. Samples for PHA and TS/VS measurements were shock-frozen in liquid nitrogen and then stored at -18°C prior to further processing. For other measurement, samples are kept in liquid form and processed immediately.

2.2.1 TS/VS

Frozen samples were lyophilized for four days until no moisture was visually observed in the sample falcon tubes. The samples were then emptied and placed in tare-weighted, small ceramic bowls and heated to 105°C in an oven for at least 12 hours. The samples were then cooled in a desiccator to room temperature and weighted after drying to determine the TS content of the sample using the following equation:

$$TS \left[\frac{g}{L} \right] = \frac{Weight_{105^{\circ}C} [g] - Weight_{ceramic} [g]}{Volume_{recorded} [L]} \quad (1)$$

After TS measurement, samples were placed in a 550°C oven for at least 2.5 hours. The samples were then cooled in a desiccator until room temperature and the weight was recorded again. VS content values were calculated with the following equation:

$$VS \left[\frac{g}{L} \right] = \frac{Weight_{105^{\circ}C} [g] - Weight_{550^{\circ}C} [g]}{Volume_{recorded} [L]} \quad (2)$$

2.2.2 PHA

Approximately 15-17mg of each lyophilized sample was placed in a glass, heat-proof vial and the weights were recorded. The amount of sample used is chosen based on the detection limit of the gas chromatography machine used and the previous PHA content observed in previous measurements. After weighting, 1mL of chloroform with 1g/L heptadecane internal standard and 1mL of acidified methanol with 20% v/v sulfuric acid was added to each vial. The samples were then placed in a 105°C oven for 3.5 hours for digestion. After digestion, the samples were cooled in an ice tray until room temperature. Then, 0.5mL of nanopure water was added and samples were vortexed for one minute to help phase-separation. The samples were left to rest overnight to allow for complete phase-separation. Thereafter, approximately 0.8 mL of the bottom phase was pipetted into a small gas chromatography (GC) vial for analysis. Each GC vial had a small molecular sieve placed within the vial to absorb residual water. The samples were run and quantified for the following monomers: polyhydroxybutyrate P(3HB), polyhydroxyvalerate P(3HV), polyhydroxy-2-methylbutyrate P(3H2MB), and polyhydroxy-methylvalerate P(3H2MV). Standards containing 0.2 mg/mL to 6.0 mg/mL for P(3HB), 0.1 mg/mL, to 1.0 mg/mL for P(3HV),

0.1 mg/mL to 1.0 mg/mL for P(3H2MB) and 0.1 mg/mL to 1.0 mg/mL were made with commercial co-polymer for calibration of the GC (GC Trace 1300, Thermo Fischer, USA). The GC was programmed to use a flame ionization detector and had a column (60m, 0.53mm internal diameter, 1 μ m film thickness) coupled with a guard-column (0.32 mm internal diameter). A helium carrier gas was used at constant pressure of 14.5 psi, injection temperature of 280°C, detector temperature of 230°C, initial temperature ramp at 40°C, increase rate of 20°C/min until 100°C, then 3°C/min until 175°C, and then 20°C until 220°C before each measurement. GC peaks were integrated at retention times of 11.52 min for P(3HB), 13.71 min for P(3HV), 12.54 min for P(3H2MB), and 14.96 min for P(3H2MV).

2.2.3 Total and Soluble Compounds

Reactor and influent samples were pre-filtered with a vacuum pump through a Millipore glass fiber filter (0.4 μ m pore size, 105 mm diameter). The filtrate was then filtered through an additional syringe charged filter (Nanofilters GF/PET 0.45 μ m, MACHEREY-NAGEL, Germany) to measure soluble compounds. sCOD, PO₄-P and NH₄-N were measured using Dr. Lange (Hach, Germany) quick tests relying on spectrophotometry. For total compounds, unfiltered samples were homogenized for 30 seconds at 20000 rpm before processing. TP and TCOD were also measured using Dr. Lange tests. For TN, catalytic oxidation was used to determine concentration (Shimadzu TOC-L CSH, Japan).

2.2.4 VFAs

The remaining influent filtrate, after processing soluble compounds, was used for VFA analysis. This remaining filtrate (6mL) was acidified with 100 μ L of 5M HCl to inhibit microbial activity and then kept at -18°C prior to processing. Acetate, propionate, valerate, iso-valerate, iso-butyrate, and butyrate were measured using ion chromatography. Samples were diluted with nanopure water before measurement based on previous measurements to the detection range of 2-20mg/L. Standards were prepared with a known gradient of concentrations from 2-20mg/L of each interested species to calibrate prior to measurement. Iso-butyrate, previously measured on GC and determined negligible, was not measured successfully on the IC due to carbonate interference. Carbonate's peak retention time occurs at a similar time to iso-butyrate, and it is not possible to distinguish the two peaks. Due to the combined inability to assess and the previous null result, iso-butyrate is excluded from analysis.

2.3 Calculations

2.3.1 Influent calculations

Nutrient availability often dictates organism behavior and is measured in this study to see the relationship between influent feed and the PHA production process. Influent nitrogen and phosphorous nutrient availability is calculated as the ratio between particulate species (Equation 3 & 4) as well the ratio between soluble species (Equation 5 & 6) within the influent feed. Further, the ratio of pCOD is calculated in relation to TCOD (Equation 7).

$$TCOD:TN \text{ ratio} \left[\frac{mg_{COD}}{mg_N} \right] = \frac{TCOD \left[\frac{mg_{COD}}{L} \right]}{TN \left[\frac{mg_N}{L} \right]} \quad (3)$$

$$TCOD:TP \text{ ratio} \left[\frac{mg_{COD}}{mg_P} \right] = \frac{TCOD \left[\frac{mg_{COD}}{L} \right]}{TP \left[\frac{mg_P}{L} \right]} \quad (4)$$

$$sCOD:PO_4\text{-}P \text{ ratio} \left[\frac{mg_{COD}}{mg_P} \right] = \frac{sCOD \left[\frac{mg_{COD}}{L} \right]}{PO_4\text{-}P \left[\frac{mg_P}{L} \right]} \quad (5)$$

$$sCOD:NH_4\text{-}N \text{ ratio} \left[\frac{mg_{COD}}{mg_N} \right] = \frac{sCOD \left[\frac{mg_{COD}}{L} \right]}{NH_4\text{-}N \left[\frac{mg_N}{L} \right]} \quad (6)$$

$$pCOD:TCOD \text{ ratio} \left[\frac{mg_{COD}}{mg_{COD}} \right] = \frac{TCOD \left[\frac{mg_{COD}}{L} \right] - sCOD \left[\frac{mg_{COD}}{L} \right]}{TCOD \left[\frac{mg_{COD}}{L} \right]} \quad (7)$$

In addition to nutrient availability, the proportion of the two main VFA species is calculated to correlate VFA composition and resulting PHA composition (Equation 8).

$$\text{Acetate:propionate ratio} = \frac{\text{Acetate} \left[\frac{mg}{L} \right]}{\text{Propionate} \left[\frac{mg}{L} \right]} \quad (8)$$

2.3.2 Reactor calculations

After the influent, it is important to understand the loading on each of the reactors (long-term and batch) in terms nutrients input per active biomass present. Active biomass or $pCOD_{cell}$ is defined as the pCOD in the reactor, not including the total PHA content within the biomass (Equation 9-11). Therefore, first the pCOD is determined in the reactor (Equation 9). Then, the PHA content is determined and converted to mg_{COD}/L by multiplying the PHA species content by its corresponding stoichiometric chemical oxygen demand (Equation 10).

$$pCOD_{total,reactor} = TCOD \left[\frac{mg_{COD}}{L} \right] - sCOD \left[\frac{mg_{COD}}{L} \right] \quad (9)$$

$$PHA_{total} \left[\frac{mg_{COD}}{L} \right] = P(3HB) \left[\frac{mg}{L} \right] * 1.67 \frac{mg_{COD}}{mgP(3HB)} + P(3HV) \left[\frac{mg}{L} \right] * 1.92 \frac{mg_{COD}}{mgP(3HV)} + P(3H2MB) \left[\frac{mg}{L} \right] * 1.92 \frac{mg_{COD}}{mgP(3H2MB)} + P(3H2MV) \left[\frac{mg}{L} \right] * 2.10 \frac{mg_{COD}}{mgP(3H2MV)} \quad (10)$$

$$pCOD_{cell} \left[\frac{mg_{COD}}{L} \right] = pCOD_{total,reactor} \left[\frac{mg_{COD}}{L} \right] - PHA \left[\frac{mg_{COD}}{L} \right] \quad (11)$$

Then, with the active biomass determined, loading on the active biomass (long-term and accumulation reactors) is then defined as the influent nutrient concentration per active biomass (Equations 12-14). sCOD loading is also commonly referred to as food to microorganism ratio (F:M ratio, Equation 12).

$$F: M \text{ ratio or } sCOD \text{ loading } \left[\frac{mg_{COD}}{mg_{COD}} \right] = \frac{sCOD \left[\frac{mg_{COD}}{L} \right]}{pCOD_{cell} \left[\frac{mg_{COD}}{L} \right]} \quad (12)$$

$$NH_4\text{-}N \text{ loading } \left[\frac{mg_N}{mg_{COD}} \right] = \frac{NH_4\text{-}N \left[\frac{mg_N}{L} \right]}{pCOD_{cell} \left[\frac{mg_{COD}}{L} \right]} \quad (13)$$

$$PO_4\text{-}P \text{ loading } \left[\frac{mg_P}{mg_{COD}} \right] = \frac{PO_4\text{-}P \left[\frac{mg_P}{L} \right]}{pCOD_{cell} \left[\frac{mg_{COD}}{L} \right]} \quad (14)$$

To monitor the effectiveness of the long-term reactors as a viable treatment method, the amount of nutrients removed within the reactor by the biomass was calculated (Equation 15).

$$\text{Nutrient Removal } [\%] = \frac{\text{Concentration}_{influent} - \text{Concentration}_{reactor}}{\text{Concentration}_{influent}} * 100\% \quad (15)$$

PHA content and yield were calculated to determine the PHA production performance of the selected biomass. The PHA content was determined by calculating the amount of PHA per pCOD within the reactor (Equation 16). In literature, PHA content is described as a weight percentage of VSS and is calculated using the conversion factor of 1.67 g_{COD}/g_{VSS} and 1.67 g_{COD}/g_{PHA} for P(3HB), 1.92 g_{COD}/g_{VSS} and 1.92 g_{COD}/g_{PHA} for P(3HV) and 1.42 g_{COD}/g_{VSS} for the cell content (Equation 16a). The PHA yield of the selected biomass was calculated as the amount of total PHA produced per sCOD consumed (Equation 17).

$$\text{PHA Content } \left[\frac{mg_{COD}}{mg_{COD}} \right] = \frac{PHA_{total} \left[\frac{mg_{COD}}{L} \right]}{pCOD_{total,reactor} \left[\frac{mg_{COD}}{L} \right]} \quad (16)$$

$$\begin{aligned} & \text{PHA Content } \left[\frac{g_{PHA}}{g_{VSS}} \text{ or } wt\% \right] \\ &= \frac{\left(PHB \left[\frac{g_{COD}}{g_{COD}} \right] * 1.67 \left[\frac{g_{COD}}{g_{VSS}} \right] + PHV \left[\frac{g_{COD}}{g_{COD}} \right] * 1.92 \left[\frac{g_{COD}}{g_{VSS}} \right] + Cell \left[\frac{g_{COD}}{g_{COD}} \right] * 1.42 \left[\frac{g_{COD}}{g_{VSS}} \right] \right)}{PHB \left[\frac{g_{COD}}{g_{COD}} \right] * 1.67 \left[\frac{g_{COD}}{g_{PHA}} \right] + PHV \left[\frac{g_{COD}}{g_{COD}} \right] * 1.92 \left[\frac{g_{COD}}{g_{PHA}} \right]} \end{aligned} \quad (16a)$$

$$\text{PHA Yield } \left[\frac{mg_{COD}}{mg_{COD}} \right] = \frac{PHA_{total} \left[\frac{mg_{COD}}{L} \right]}{sCOD_{consumed} \left[\frac{mg_{COD}}{L} \right]} \quad (17)$$

To quantify the PHA content increase from before and after the accumulation batch tests, the relative PHA content increase was calculated by taking the initial PHA amount (PHA_{total,initial}) at the beginning of the batch and maximum PHA amount during the batch (PHA_{total,max}) (Equation 18).

$$\text{Relative PHA increase } [\%] = \frac{PHA_{total,max} - PHA_{total,initial}}{PHA_{total,initial}} \quad (18)$$

Intracellular nitrogen (iN) and phosphorous (iP) content were also calculated (Equation 19 & 20). The amount of N and P within the active biomass can be used as an indicator for biomass population type. Differing microorganism species composition often come with a shift in iN or iP

value. Understanding the relationship between iN/iP and PHA content and yield can be beneficial for maximizing PHA content.

$$iN = \frac{TN[\frac{mg_N}{L}] - NH_4-N[\frac{mg_N}{L}]}{pCOD_{cell}} \quad (19)$$

$$iP = \frac{TP[\frac{mg_P}{L}] - PO_4-P[\frac{mg_P}{L}]}{pCOD_{cell}} \quad (20)$$

Another metric that can influence the selection pressure for PHA-storers is the ratio between the feast phase (period where VFA substrate is available for consumption) and the overall cycle time which includes the famine phase (period where VFA substrate is depleted) (Equation 21).

$$Feast\ Fraction\ (FF)[\%] = \frac{Time_{feast}[s]}{Time_{feast}[s] + Time_{famine}[s]} \quad (21)$$

As mentioned previously, the reactors were cleaned twice per week to scour and remove biofilm from the reactor walls. Biofilms inhibit the measurement campaign because they consume nutrients which are not visualized by the sampling methodology; uniform samples were taken from the suspended fraction of the reactors and the biofilm was not considered. This is done because in practice, on the plant-scale, biofilm surface area is much smaller in proportion to the volume of the reactor tank used so biofilm influence would be negligible. Due to the much smaller reactor size on the lab scale, the biofilm may play a significant role in PHA metrics recorded. To measure the influence of biofilm presence on the PHA content, the ratio of TP in the influent to TP in the reactor was used as an indicator (Equation 22). TP should remain constant between influent and the reactor and difference between the two was assumed to be due to biofilm interference.

$$Biofilm\ Fraction\ (BF)[\%] = \frac{TP_{reactor}[\frac{mg}{L}]}{TP_{influent}[\frac{mg}{L}]} \quad (22)$$

3 Results

3.1 Influent feed composition

The reactor influent composition was monitored throughout the experiment (Table 2, Figure 6, Figure 7). VFA's represented $87\% \pm 6\%$ and $84\% \pm 12\%$ of the influent sCOD before and after solids removal, respectively. Propionate was the dominant acid throughout the entire experiment, accounting for roughly 80% of the total VFAs (Table 2).

Installation of the membrane allowed to successfully remove particles from the fermented broth: the pCOD:TCOD ratio decreased from $48\% \pm 5\%$ (no membrane) to $12\% \pm 6\%$ (with membrane) (Figure 6). The remaining non-VFA fraction of the overall sCOD amounted to 400 ± 191 mg/L before solids removal and reduced to 242 ± 194 mg/L after solids removal. VFA species fluctuate

throughout the entire experiment and are primarily due to variations in the primary solids being supplied from Eawag WWTP to the anaerobic digester (Table 2). To characterize differences between the phases, VFA concentration decreased for all VFA species after solids removal. There was a 50% reduction in total VFAs in the influent (Table 2). Also, concentration of all VFA species fluctuated less in proportion to the average value after solids removal. When looking at the percentage of each VFA species, composition remained similar before and after solids removal. The main difference observed is a 46% decreased share of acetate with much less fluctuation and an increase of 47% and 13% of iso-valerate and valerate, respectively, after solids removal.

Table 2: Influent composition in terms of concentration and percentage of total VFA before and after the removal of solids by ultrafiltration.

		Influent VFA composition [mg _{COD} /L or %]					
		Total VFA	Acetate	Propionate	Butyrate	Isovalerate	Valerate
Conc. [mg _{COD} /L]	Before	2777 ± 1078	271 ± 369	2108 ± 762	174 ± 60	94 ± 42	132 ± 58
	After	1390 ± 364	48 ± 14	1098 ± 340	101 ± 25	73 ± 18	73 ± 18
% of Total VFA	Before	100	8.2 ± 8.9	77.0 ± 8.0	6.4 ± 1.1	3.6 ± 1.4	4.8 ± 1.0
	After	100	3.8 ± 1.5	78.1 ± 5.5	7.6 ± 2.3	5.3 ± 1.7	5.4 ± 1.0

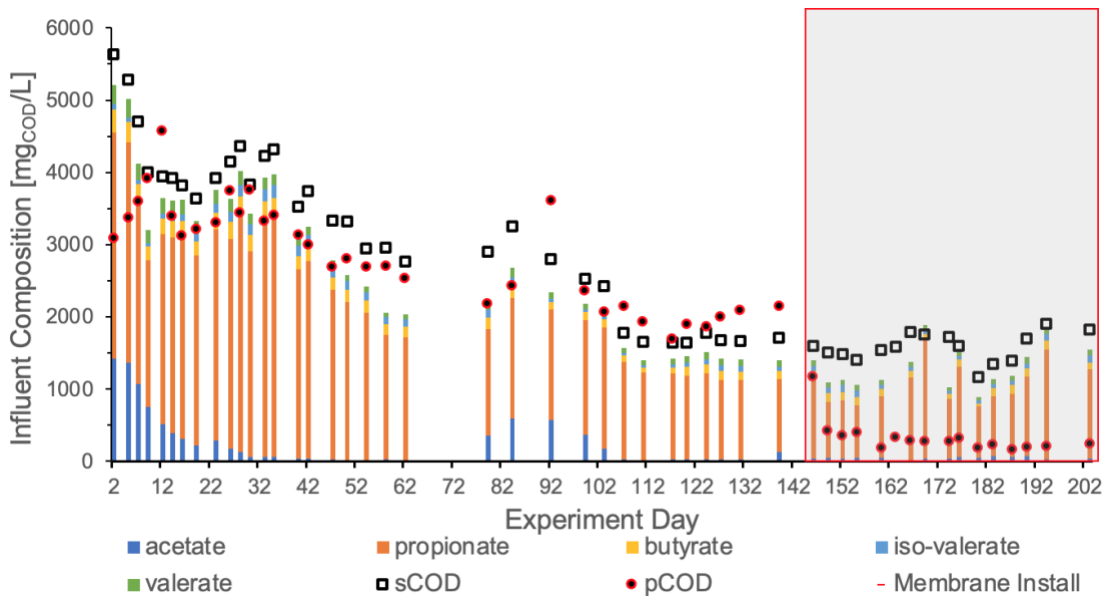


Figure 6: Evolution of influent composition before and after solids removal (red box): infeed is dominated by propionate before and after solids removal. The key difference after solids removal is the decreased presence of pCOD.

The influent was characterized by a change in nutrient availability before and after solids removal. Nitrogen availability represented by the TCOD:TN ratio increased by 92% from 34.6 ± 4.8 to 66.3 ± 31.6 g_{COD}/g_N while phosphorous availability represented as TCOD:TP ratio decreased by 26% from 131.9 ± 30.3 to 97.6 ± 34.3 g_{COD}/g_P (Figure 7). TCOD:TN and TCOD:TP ratio were both significantly different before and after solids removal (p-value = 0.0006 and p-value = 0.0003,

respectively). Ratios of greater than 20 $\text{g}_{\text{COD}}/\text{g}_{\text{N}}$ and 100 $\text{g}_{\text{COD}}/\text{g}_{\text{P}}$ are limiting for typical PHA biomass (Wen et al., 2010). Therefore, it was expected that mainly nitrogen would be limiting for growth according to this study's influent composition.

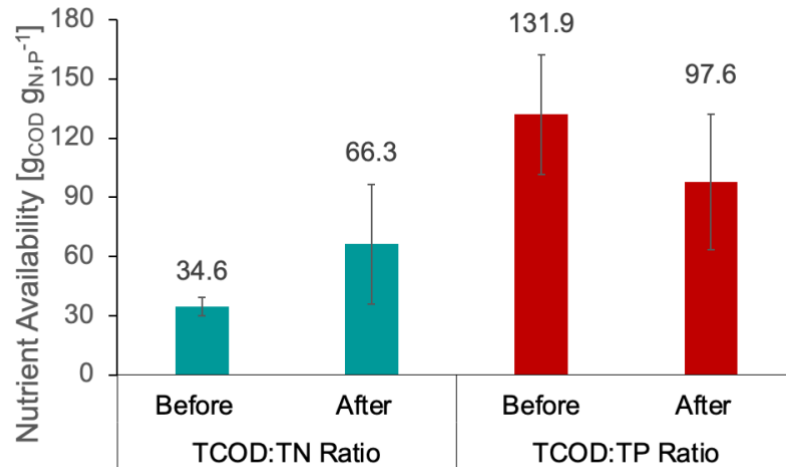


Figure 7: Influent nitrogen and phosphorous nutrient availability before and after solids removal.

3.2 Long-term reactor performance

Both reactors function as successful wastewater treatment methods, removing almost all incoming sCOD, $\text{NH}_4\text{-N}$, and $\text{PO}_4\text{-P}$ before and after the filtration of solids from the influent (Table 3: Reactor treatment capabilities represented by low effluent concentration of nutrients and high removal efficiency. Table 3). No VFAs were detected in the effluent of the SBR and the CSTR, indicating a full removal of biodegradable sCOD. Thus, effluent sCOD likely consisted of non-biodegradable material. After solids removal, phosphorous removal decreased slightly by 11% for the SBR and 4% in the CSTR. Nitrogen removal remained high with decreased fluctuation after solids removal. Phosphorous concentration remained below 1.0 mg/L for both reactors before solids removal and increased slightly with more fluctuation after solids removal. Nitrogen concentration remained below 0.2 mg/L before solids removal for both reactors and increased after solids removal with more fluctuations. In terms of environmental growth conditions, for both the SBR and the CSTR, nitrogen availability was on average greater than 1000 $\text{g}_{\text{COD}}/\text{g}_{\text{N}}$ before solids removal. After solids were removed, nitrogen availability was also on average greater than 1000 $\text{g}_{\text{COD}}/\text{g}_{\text{N}}$ for the CSTR and 300 $\text{g}_{\text{COD}}/\text{g}_{\text{N}}$ for the SBR (end of famine phase).

Table 3: Reactor treatment capabilities represented by low effluent concentration of nutrients and high removal efficiency. Effluent refers to the samples taken during the decant or end of famine phase for the SBR and refers to the continuous outflow for the CSTR.

		Effluent Concentration [mg/L]		Removal Efficiency [%]	
		SBR	CSTR	SBR	CSTR
sCOD	Before	194 ± 91	203 ± 49	93 ± 3	93 ± 3
	After	190 ± 130	153 ± 77	89 ± 9	92 ± 5
PO₄-P	Before	0.87 ± 0.46	0.93 ± 0.50	93 ± 6	92 ± 9
	After	2.24 ± 1.59	1.76 ± 1.03	83 ± 13	88 ± 7
NH₄-N	Before	0.15 ± 0.13	0.11 ± 0.08	99 ± 2	97 ± 14
	After	0.62 ± 1.66	0.13 ± 0.17	99 ± 2	99 ± 1

3.2.1 PHA content and composition of reactor biomass

The average PHA content in the SBR biomass was similar during both experimental phases: 0.20 ± 0.10 g_{COD}/g_{COD} without and 0.17 ± 0.06 g_{COD}/g_{COD} with filtration of the influent (Figure 10). PHA composition shifted after solids removal from being P(3HV) dominated to P(3HB) dominated (Figure 8, Figure 10, Table 4). Average PHB:PHV ratio for the SBR increased 41% from before solids removed to after solids removed and is statistically different (p-value = 0.02). SBR P(3HV) fluctuated more frequently before solids removal and P(3HB) fluctuated more frequently after solids removal. End of cycle PHA content was not much lower than end of feast PHA content for the SBR. PHA yield remained statistically the same for the SBR after solids removal (0.09 and 0.07 g_{COD}/g_{COD}, p-value < 0.01) (Figure 11).

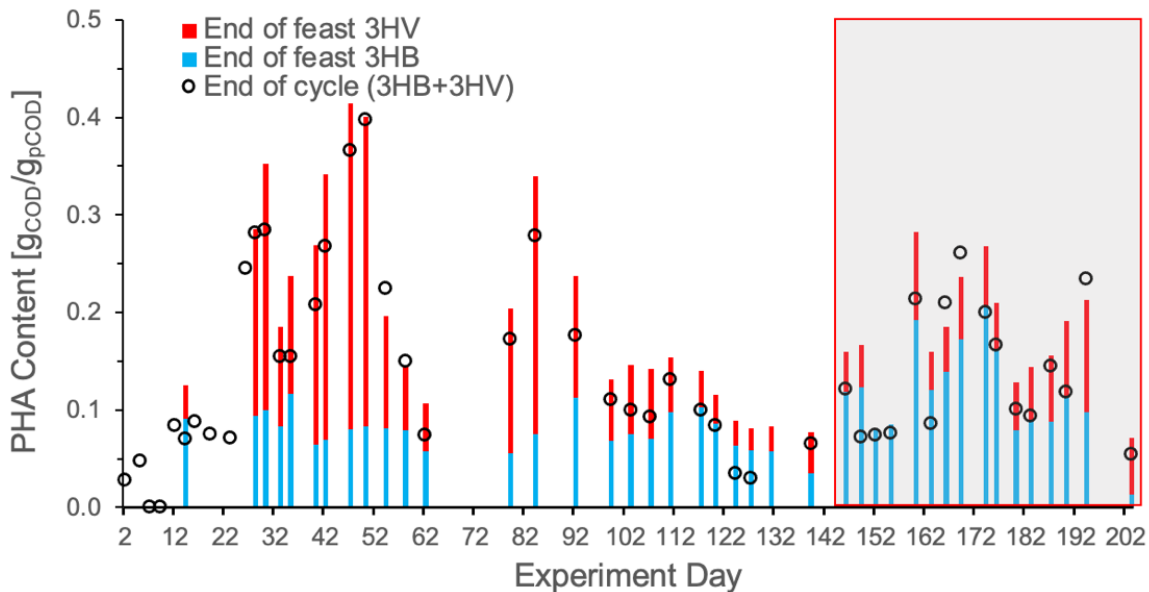


Figure 8: SBR PHA content at the end of feast phase represented by blue bars for P(3HB) and red bars for P(3HV), the red box indicates the time period after the removal of solids from the

influent and the black circles represent the total PHA measured at the end of cycle or famine phase.

The average PHA content in the CSTR biomass changed significantly, increasing by 240% after solids removal but remained highly variable. In terms of PHA composition, the CSTR did not have a significant change in P(3HB):P(3HV) ratio (p -value = 0.35) (

Figure 9, Figure 10, Table 4). Absolute P(3HV) and P(3HB) content both increased after solids removal (

Figure 9). PHA yield decreased significantly for the CSTR after solids removal (Figure 11).

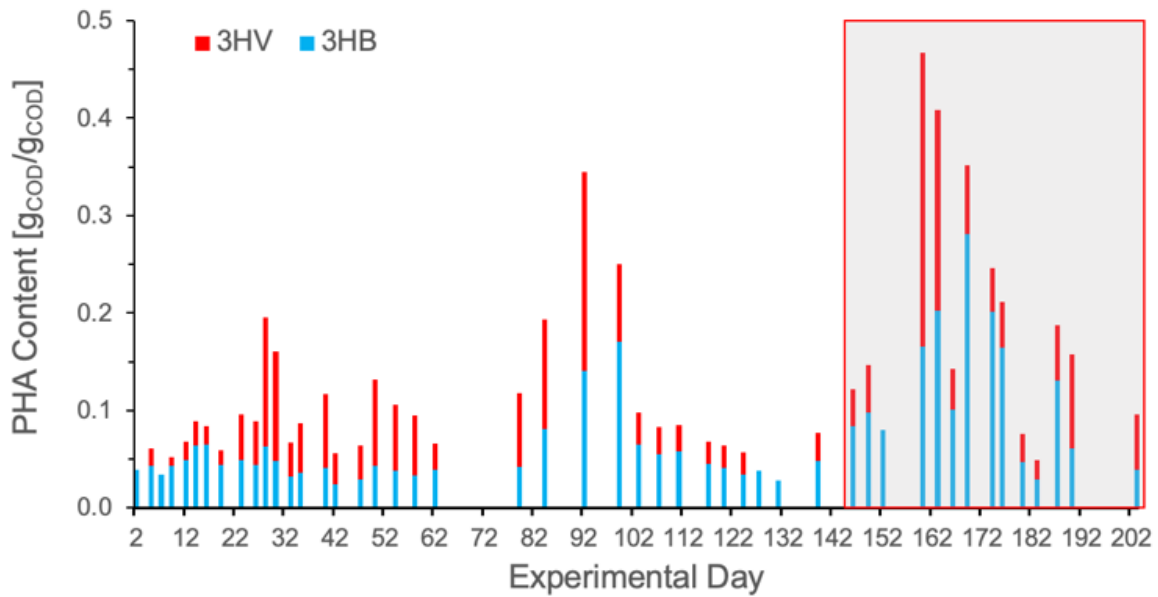


Figure 9: CSTR PHA content with blue bars representing P(3HB) and red bars representing P(3HV), the red box indicates the time period after the removal of solids from the influent.

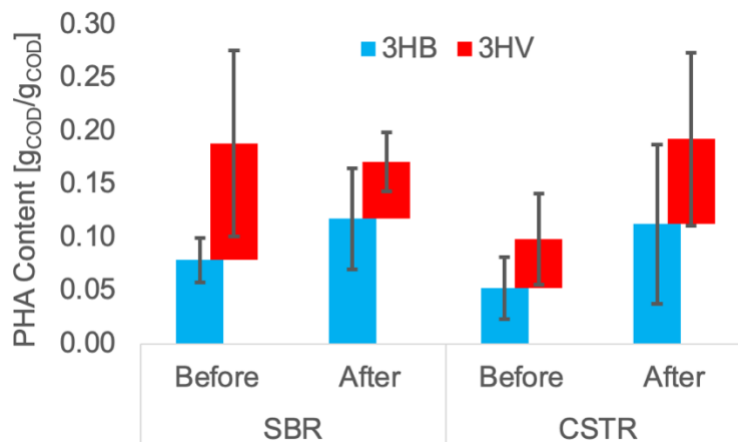


Figure 10: Average SBR and average CSTR PHA content separated by PHA species before and after solids removal. Bars are offset to avoid overlapping error bars. For the SBR, the two

average values are not significantly different (p -value = 0.26). However, the CSTR averages are significantly different (p -value = 0.01) with a 240% increase after solids removal.

Table 4: SBR and CSTR PHA content by species type and the ratio between P(3HB) and P(3HV) before and after solids removal.

		P(3HB)	P(3HV)	P(3HB):P(3HV)
SBR	Before	0.08 ± 0.02	0.11 ± 0.09	1.28 ± 0.90
	After	0.12 ± 0.05	0.05 ± 0.03	2.16 ± 0.95
CSTR	Before	0.05 ± 0.05	0.05 ± 0.04	1.53 ± 0.99
	After	0.11 ± 0.08	0.08 ± 0.08	1.93 ± 1.31

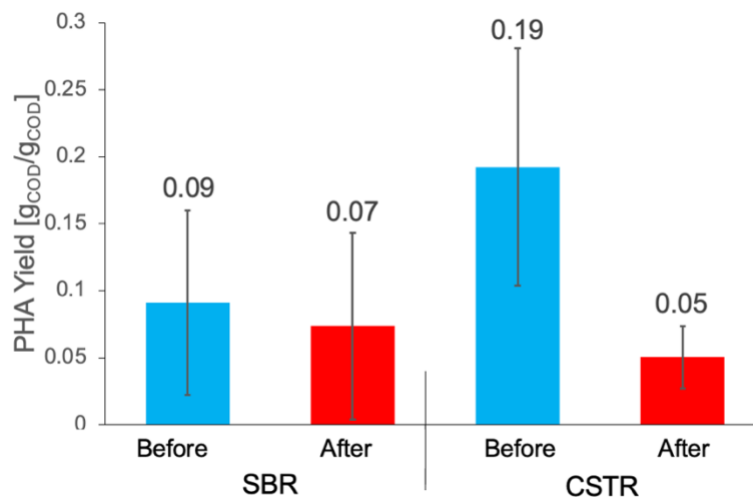


Figure 11: Average SBR and CSTR PHA yield before and after solids removal. For the SBR, the two average values are not significantly different (p -value = 0.43). However, the CSTR averages are significantly different (p -value = $9e-9$) with a 74% decrease after solids removal.

To understand the dynamics between influent loading and the reactor loading on the PHA content and composition, a spearman correlation matrix was created to identify possible connections (Figure12a and 12b). Spearman correlation values represent the extent to which a monotonic function can describe the relationship between two variables. It is important to note that correlation does not necessary imply that the factors are connected causally and there may be an outside confounding variable for all relationships. Also, it is important to note that sample size for correlation is smaller after solids removal than before solids removal (16 after vs. >26 before). When comparing the two systems **before** the influent solids removal, the strongest and most significant correlations include the following:

- **PHA Content:**
 - For SBR, the influent parameter acetate/propionate ratio is negatively correlated with increasing PHA content.
 - In contrast, the CSTR had no influent conditions correlating with PHA contents.

- For SBR, the reactor condition $\text{NH}_4\text{-N}$ and $\text{PO}_4\text{-P}$ load on the active biomass, as well as intracellular N/P is positively correlated with increasing PHA content. Further, the feast fraction of the SBR cycle is positively correlated with increasing PHA content.
- In contrast, the CSTR had no reactor conditions correlating with PHA contents.
- **PHA Composition:**
 - For SBR, influent characteristic soluble sCOD: $\text{NH}_4\text{-N}$ ratio was found to be positively correlated with increased PHB/PHV ratio.
 - For the CSTR, influent characteristic acetate/propionate ratio and TCOD:TN ratio was found to be most positively correlated with increasing PHB/PHV ratio.
 - For SBR reactor conditions, the nutrient loading of $\text{NH}_4\text{-N}$, sCOD, and $\text{PO}_4\text{-P}$ on the active biomass in the reactor all correlated positively with increased PHB/PHV ratio.
 - For the CSTR, only the reactor condition of intracellular N was found to be negatively correlated with PHB/PHV ratio.

When comparing the two systems *after* influent solids removal, the strongest, most significant correlations include the following:

- **PHA Content:**
 - Similarly to the phase before removal of influent solids, only one influent condition held a significant link with the PHA content in the SBR: the acetate/propionate ratio correlated negatively with the PHA content.
 - When compared to the CSTR, only influent TCOD:TN ratio was strongly positively correlated with PHA content.
 - Further, for SBR reactor conditions, $\text{NH}_4\text{-N}$ loading on the active biomass and intracellular N content had the strongest negative correlation with PHA content. SBR reactor conditions, $\text{PO}_4\text{-P}$ loading, sCOD loading, intracellular P, and feast time all had significant positive correlation with PHA content.
 - For CSTR reactor conditions, it was like the SBR: increased sCOD loading was also strongly positively correlated with PHA content, $\text{PO}_4\text{-P}$ loading was slightly positively correlated with PHA content as well, and intracellular P was also positively correlated.
- **PHA Composition:**
 - Regarding the SBR, only one significant link could be observed between the PHB/PHV ratio and the influent composition: a negative correlation with the TCOD:TP ratio.
 - For the CSTR, TCOD:TN ratio and sCOD: $\text{NH}_4\text{-N}$ ratio were positively correlated. Acetate/propionate ratio was slightly negatively correlated.
 - For SBR reactor conditions, there were no significant correlations.
 - For CSTR reactor conditions, intracellular N was positively correlated with PHB/PHV ratio.

In general, the main findings from the spearman correlation matrix show that the SBR and CSTR have entirely different correlations and correlation strengths before solids removal. After solids

removal, the SBR and CSTR have mostly the same correlation direction but different strengths and significance. Generally, the SBR is more correlated with loading on the active biomass and the CSTR is more significantly correlated with influent nutrient availability.

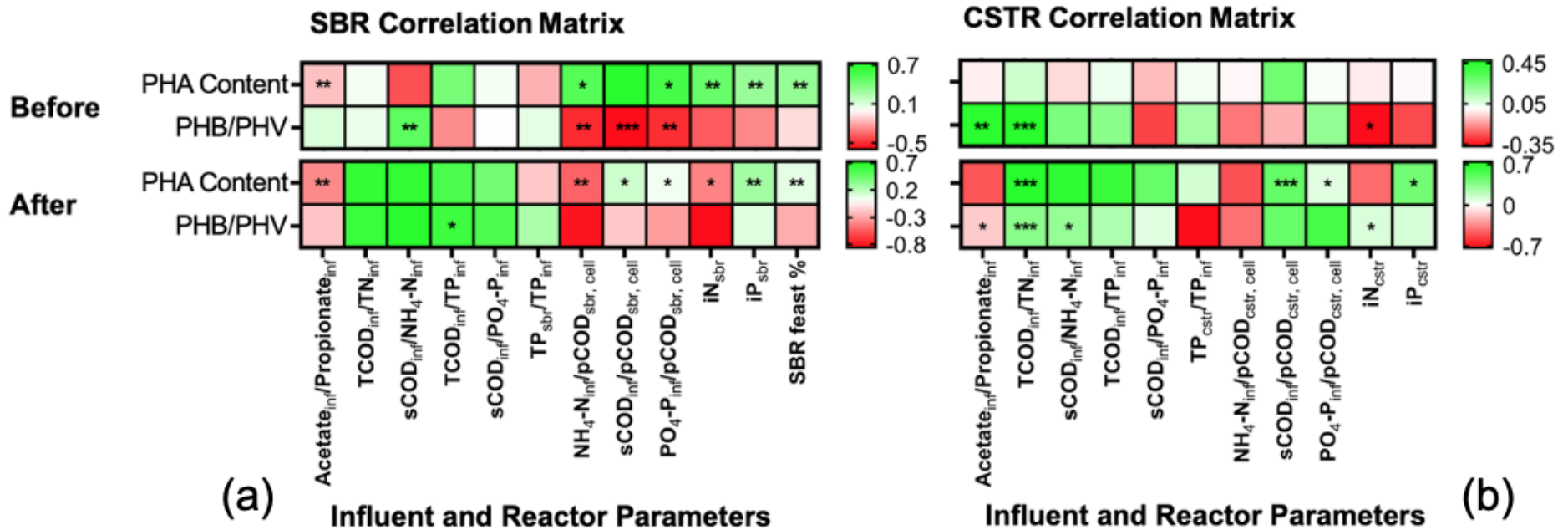


Figure 12: SBR (a) and CSTR (b) correlation matrix showing the spearman correlation between influent/reactor parameters and PHA content/composition. Darker green shaded boxes indicate increasing positive correlation, darker red shaded boxes indicate increasing negative correlation, and white boxes indicate no correlation. Stars indicate p-value significance with * meaning p-value < 0.05, ** for p-value < 0.01, and *** for p-value < 0.001.

3.3 Accumulation batch results

Accumulation batches resulted in higher PHA content within the selected biomass than the PHA content observed in the long-term selection reactors for all batches and for both reactors (Figure 11 & 12). Batches one to four were completed before this study and are positioned to compare with batch five and six completed in this study.

For the SBR, the last batch on day 197 contrasts two reactor conditions, one accumulation reactor containing $\text{NH}_4\text{-N}$ limited availability at 0.5 mg/L and a sCOD:N ratio of 2500 $\text{g}_\text{C}/\text{g}_\text{N}$ while the other reactor contained $\text{NH}_4\text{-N}$ excess availability at 100 mg/L and a sCOD:N ratio of 15 $\text{g}_\text{C}/\text{g}_\text{N}$ (Figure 13). No significant differences were observed in the maximum PHA content with or without $\text{NH}_4\text{-N}$.

For the CSTR (Figure 12), the last batch on day 204 similarly contrasts two reactor conditions, one reactor with $\text{NH}_4\text{-N}$ excess availability at 100 mg/L and a C:N ratio of 15 $\text{g}_\text{C}/\text{g}_\text{N}$ while the other reactor contained $\text{NH}_4\text{-N}$ limited availability at a concentration of 0.1 mg/L and a C:N ratio of 15000. Contrary to the SBR, the maximum PHA content decreased by 56% with the presence of $\text{NH}_4\text{-N}$ excess, indicating that nitrogen availability may be a governing factor in storage response for the CSTR.

When comparing the batches completed in this study to the batches completed in previous work at Eawag before solids removal, PHA content remained similar for the SBR when looking only at batch three and four compared to five and six. Batch one and two achieved much higher PHA content. When comparing batches before and after solids removal for the CSTR, PHA content decreased. When comparing maximum PHA content in the accumulation batches after solids removal between the SBR and CSTR, the SBR performed better with 31% more PHA content. However, for yield, SBR and CSTR had identical maximum yield of 0.2 $\text{g}_{\text{COD}}/\text{g}_{\text{COD}}$. For PHA composition, the SBR produced more P(3HB) than P(3HV) while the CSTR produced the exact opposite.

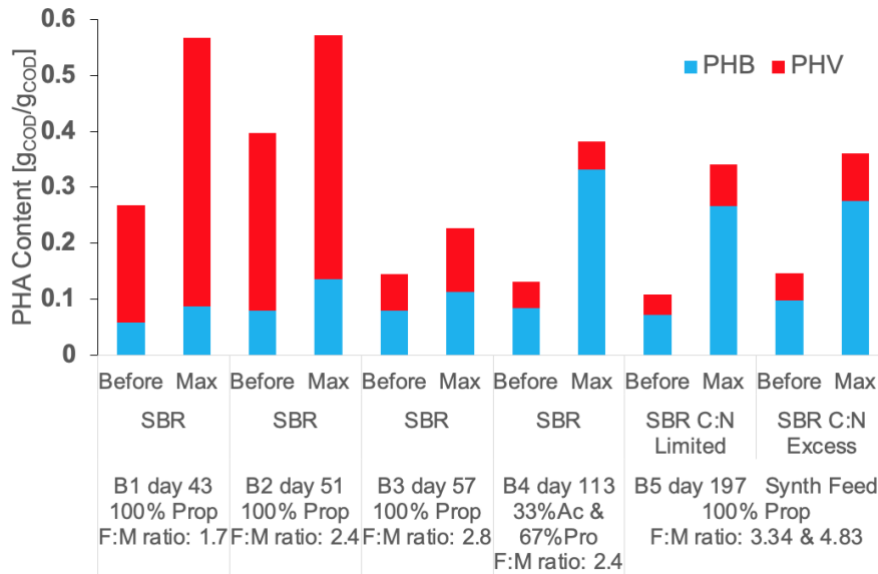


Figure 13: SBR PHA content and composition at the start and at the maximum value of accumulation batches (PHB is P(3HB), PHV is P(3HV)).

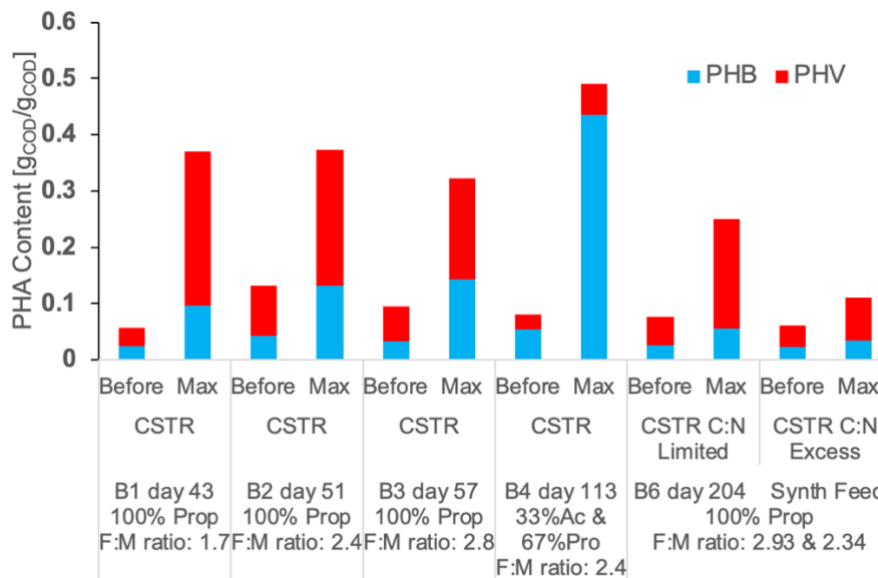


Figure 14: CSTR PHA content and composition at the start and at the maximum value of accumulation batches (PHB is P(3HB), PHV is P(3HV)).

PHA yield was greater in the accumulation reactor batches when compared to the sampling day before of the long-term selection reactors (Figure 13 & 14). PHA yield decreased with the removal of solids in the last batch for both the SBR and the CSTR. For the last batch, the effect on nitrogen availability had different outcomes. The SBR maximum yield during the accumulation batch increased by 45% in the presence of excess $\text{NH}_4\text{-N}$ (Figure 13) while the maximum yield decreased by 47% for the CSTR (Figure 14).

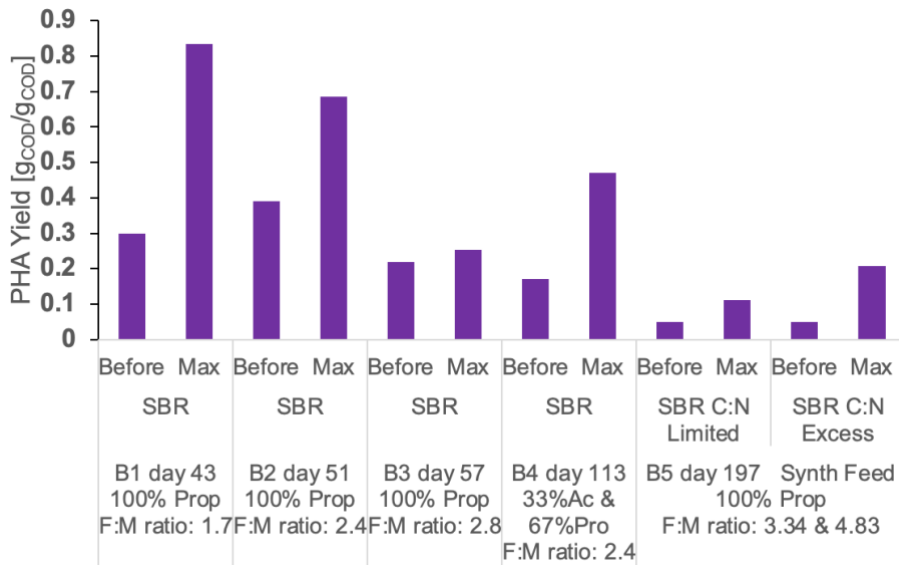


Figure 15: SBR PHA yield the sampling day before and on the day of the accumulation batch.

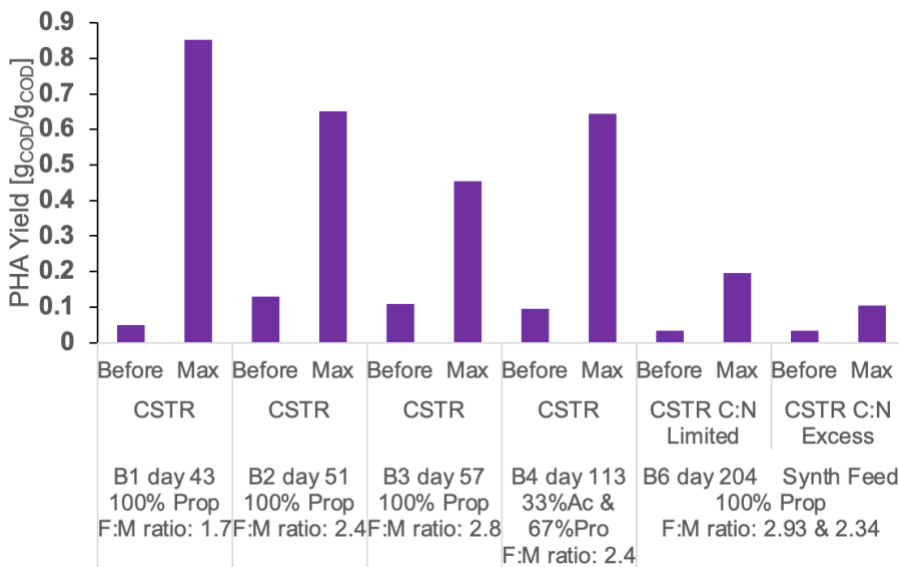


Figure 16: CSTR PHA yield the sampling day before and on the day of the accumulation batch.

The accumulation batches tested had different nitrogen availability and C:N ratios ranged from 15 to above 15000. Lower nitrogen availability was associated with increased relative PHA gain for both the SBR (Figure 15a) and the CSTR (Figure 15b). Stronger correlation strength was found for the CSTR than the SBR indicating that nitrogen availability may be a stronger governing factor for storage for the CSTR and less so for the SBR.

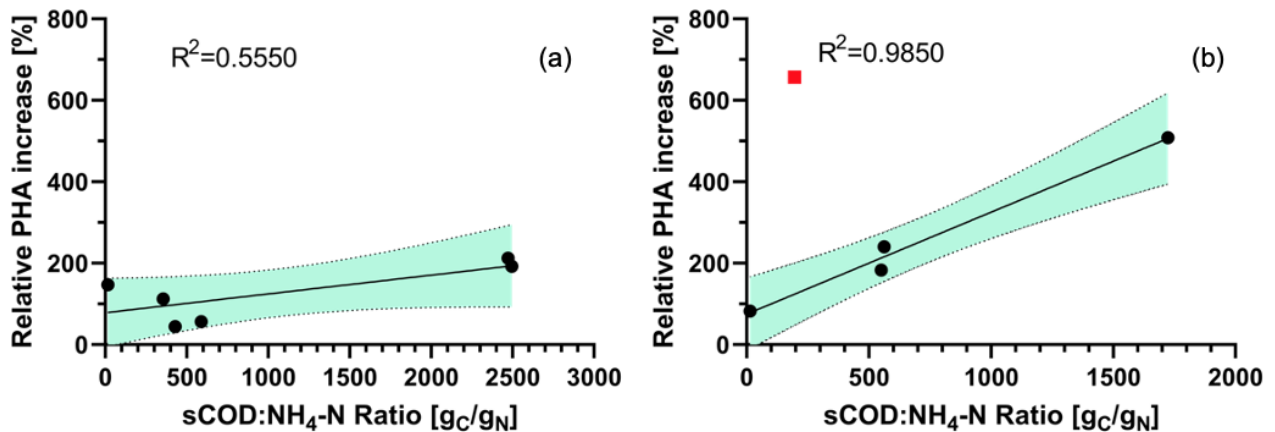


Figure 17: SBR (a) and CSTR (b) Relative PHA increase percentage during accumulation batches as a function of initial nitrogen availability. Two points outside of the 95% confidence interval are excluded for the CSTR.

4 Discussion

4.1 Effect of removal of solids on PHA content and yield

The removal of particulates directly impacts the PHA content values being calculated and was expected to have the effect of correcting the potential underestimation of PHA content explained in the previous work at Eawag before solids removal (Bettex, 2021). Underestimation was expected in the previous work because PHA content values contained biomass pCOD and recalcitrant pCOD incoming from the influent, resulting in dilution of PHA content value. However, contrary to expectation, average PHA content for the SBR decreased both in the selection reactor and in the accumulation batch test. This is hypothesized to be because of worse selection in the reactor or changing influent and reactor environmental conditions. For the CSTR, the expected effect was observed in the long-term selection reactor, but upon testing in the accumulation reactor, maximum PHA values were also lower than observed before solids removal. Similar to the SBR, this suggests that influent composition change, changing environmental conditions, and/or worse selection occurred in the CSTR too.

Another impact of the removal of solids was the decreased number of influent particulates available for hydrolysis. This was suspected to have a non-negligible effect on PHA content and yield. The hypothesis from previous work suggested that the selected biomass used hydrolyzed particulate nutrients to synthesize PHA and this was not captured in the PHA yield metric which only considered consumed soluble carbon substrate (Bettex, 2021). This is reinforced in this study after solids removal where decreased PHA yield values were observed. However, this decreased PHA yield value may be solely the result of worse selection. It is not known the extent to which PHA yield value decrease is attributed to particulate hydrolysis, worse selection, or another external condition.

4.2 Selection within the reactors: SBR vs. CSTR

The presence of selection is clear amongst both the SBR and the CSTR before and after solids removal. This is demonstrated by the relative increase in PHA content observed during *all* accumulation batch tests for *both* reactor biomasses. Poor selection of PHA-storers would show low or no PHA content during accumulation batch testing. This continues to validate the findings found from previous research at Eawag which showed selection in both reactor modes with comparable storage potentials of 45 and 34 wt% PHA for the SBR and CSTR, respectively (Bettex, 2021). Before solids removal, the SBR had higher storage compared to the CSTR. After solids removal, this finding remains with the SBR having a storage potential of 33 wt% PHA compared to the CSTR with 21 wt% PHA.

As discussed in previous work at Eawag, the SBR was able to select for PHA organisms through transient carbon availability (Bettex, 2021). This governing condition created a cycle of interchanging feast and famine phases that favored the selection of PHA storers. Many studies previously have discussed this as a driving force for selection (Valentino et al., 2017). The current highest PHA content recorded with a pilot-scale SBR and real wastewater from the organic fraction of municipal solid waste has been 77 wt% PHA (Michel et al., 2020). In another study, fed with synthetic wastewater and an SBR selected biomass, maximum PHA content reached even greater values of 85 wt% PHA (Johnson et al., 2009). In general, PHA content has ranged from 0.17 to 0.85 wt% PHA for SBR operated studies (Bettex, 2021; Estévez-Alonso et al., 2021). Results in this study (33 wt% PHA). were significantly lower than the highest values found within literature but remained within the wide range of what is typically observed. One critical aspect of SBR selection mechanism is the ability of the selected PHA storers to grow on stored carbon during the famine phase. This was inhibited when there was less nitrogen availability and a higher TCOD:TN ratio after solids removal (92% increase from 34.6 to 66.3 g_{COD}/g_N). In literature, lower nitrogen availability has been associated with decreased ability to select for PHA storers within an SBR (Albuquerque et al., 2007; Kleerebezem et al., 2015; Reis et al., 2011). It is also suggested in literature that low nitrogen availability during the feast phase limits the growth of the PHA storers during the proceeding famine phase resulting in a less effective selection.

For the CSTR, the mechanisms are different from the SBR. The effluent concentrations show that the CSTR has consistently low amounts of nitrogen available (0.11 ± 0.08 mg_N/L before solids removal and 0.13 ± 0.17 mg_N/L after solids removal). This suggests that there is always a nitrogen limitation within the CSTR even after solids removal. Further, no VFAs were detected within the CSTR suggesting a dual limitation as a potential cause for selection. Few studies have been completed using real wastewater and a CSTR process scheme. One previous study achieved 61 wt% PHA with a CSTR selected biomass and synthetic wastewater (Albuquerque et al., 2010). This previous study suggested the premise of dual nutrient limitation (carbon and phosphorous) for the selection of PHA-storers within a CSTR. However, as stated in previous research at Eawag, it is not possible to distinguish whether dual carbon and nitrogen limitation is the selection mechanism or the trigger for storage (Bettex, 2021). An essential point of this study was to dive deeper into the nitrogen availability, to determine if it is a trigger for storage in addition to the possibility of it as a selection mechanism. With only one study with a CSTR selection reactor in literature, it is difficult to position the CSTR results found in this study. Nonetheless, PHA content

achieved in this study after solids removal (21 wt% PHA) is low but within range of PHA content observed for all PHA production schemes (Estévez-Alonso et al., 2021).

Overall, after solids removal, maximum PHA content values show that selection was not optimal in both reactors. PHA content was on the lower end of values typically found in literature and low compared to values found before solids removal for both the SBR and the CSTR. Furthermore, for the SBR, PHA content at the end of cycle was similar to the PHA content at the end of the feast phase. This indicates low activity and growth on stored PHA which suggests poor selection of storers. While the results in this study point towards poor selection, it is still important to consider the possibility that the influent and reactor conditions may be the explanation for different storage responses.

Looking at influent parameters and reactor environmental conditions are the next logical step for understanding the decreased PHA output observed. Throughout the phase where solids were removed, influent conditions changed frequently, and it is difficult to visualize the impact of the constant changes. The spearman correlation matrix within this study showed that many factors could impact the PHA content and composition for both the SBR and the CSTR and its findings are discussed in the subsequent section.

4.3 Link between influent composition, selection of storing organisms, and PHA storage

The spearman correlation matrix shows **different** correlations and correlation strengths between the SBR and CSTR before solids removal. Contrastingly, after solids removal, this changes and correlation direction is **similar**, but strengths are different. One potential reason that could explain this pattern could be the hydrolysis of particulates. The SBR and CSTR may have had different hydrolysis capabilities leading to diverting correlations and strengths. However, after solids removal, this was no longer a factor leading to more homogenized correlations between the two reactors. Findings *after* solids removal will be prioritized for discussion since the effect of hydrolyzed particles will be reduced.

After solids removal, the spearman correlation matrix showed the SBR to be more affected by loading parameters and the CSTR to be more affected by influent nutrient availability. This could be due to the different selection mechanism between the two reactors. The SBR selection is based on transiency therefore loading becomes more influential. Without sufficient loading, PHA storers cannot grow on stored PHA inhibiting selection and therefore storage as well. For the CSTR, selection is hypothesized to be due to carbon and nutrient limitation therefore it is logical that influent nutrient availability would play a larger role.

4.3.1 Spearman correlation matrix: PHA content

From the spearman correlation matrix, we see that acetate to propionate ratio is significantly negatively correlated with PHA content in the SBR. This may be because the selection reactors are mostly exposed to propionate. This would favor selection of propionate synthesizing species and therefore content would be higher in presence of lower acetate to propionate ratio. This

observation is not significantly demonstrated for the CSTR suggesting that the CSTR may have quicker adaptation to changing VFA composition change.

The spearman correlation matrix also shows that carbon loading has a strong positive correlation with increasing PHA content in the SBR while nitrogen loading is negatively correlated. The same findings are seen in the CSTR. This further enforces previous studies which have indicated that optimal storage occurs under excess carbon and growth limiting loading conditions (Rhu et al., 2003).

iN and iP are negatively and positively correlated with SBR PHA content, respectively. For the CSTR, similar correlation direction is seen but with less significance. This suggests that the CSTR has higher adaptability to changing influent conditions as the PHA content is less dependent on microorganism iN and iP. This is the opposite for the SBR, which is more sensitive to changing iN and iP.

For the SBR, feast fraction percentage had a significant but weak positive correlation with PHA content. This is opposing to literature which states that increase in feast fraction is usually associated with worse selection (Reis et al., 2011). This is hypothesized to be because when the famine phase is too short, there is not enough selection pressure to incentivize high storage (Beccari et al., 1998). One potential reason for the conflicting correlation found in this study may be that the relationship between feast percentage and PHA content is not linear. It could be that increasing feast length may be beneficial up to a specific threshold and only inhibitory after going above this threshold.

For both the SBR and the CSTR, nitrogen availability expressed in TCOD:TN is positively correlated with PHA content. It is, however, much more significantly correlated for the CSTR. This iterates the higher association of CSTR PHA content with low nitrogen availability. However, as stated before it is not clear whether this is solely a factor leading to better selection, a trigger for storage or both.

4.3.2 Accumulation batch test: PHA content

To be able to clarify if nitrogen limitation is a governing factor for storage, two sub-batches with and without ammonium in the influent were done for both reactor biomasses. The batch tests showed a clear difference between the SBR and CSTR: the SBR maximum PHA content remained the same regardless of nitrogen availability while the CSTR maximum PHA content decreased with nitrogen present in excess. Therefore, nitrogen limitation is potentially a governing factor in PHA storage for the CSTR and not so for the SBR. One caveat to this comparison batch test is the feeding regime. Both reactor batch tests comparing nitrogen availability also had a carbon gradient. Therefore, it not possible to distinguish the extent to which nitrogen availability or carbon gradient governed storage. Future CSTR batch tests should be completed with a continuous feeding strategy to remove the effect of the transient carbon supply. The finding of nitrogen availability affecting PHA storage is further reinforced when looking at the relative PHA gain in Figure 17. The CSTR has a much stronger and significant correlation with nitrogen availability compared to the SBR. This could be due to the different selection mechanisms between the SBR and the CSTR. Within the SBR, the biomass is exposed to nitrogen excess

each cycle at the beginning and may not be accustomed to batch tests with strong nitrogen limitation. This is in contrast to the CSTR where the biomass is constantly exposed to a nitrogen limited environment.

Previous studies have shown that food to microorganism ratio also plays a role in the synthesis of PHA. PHA storage increases with increasing food to microorganism ratio up until a specific concentration to which the feast phase is too long and the famine phase is too short to select for storers (Thompson et al., 2010). Feast to famine ratio was the highest in the batches after solids removal and may also explain partially the decreased PHA content values.

4.3.3 Spearman correlation matrix: PHA composition

Composition is similar between the two selection reactors with both being mostly P(3HB) rather than P(3HV) on average (2.16 ± 0.95 and 1.93 ± 1.31 gP(3HB)/gP(3HV), SBR and CSTR, respectively). As mentioned previously, acetyl-CoA is the main precursor for P(3HB) however, propionyl-CoA can also be transformed to P(3HB) by decarboxylation to acetyl-CoA. This mechanism most likely occurs within both selected biomasses because the acetate VFA fraction is not high enough to be the sole source of PHB (4% acetate, 57% PHB in CSTR, 70% in SBR). Within the spearman correlation matrix, this pattern is supported for both the CSTR and SBR. Acetate/propionate ratio is negatively correlated with P(3HB):P(3HV) ratio indicating that decarboxylation is a dominant pathway within both reactors are solids removal. This could be due to a number of reasons including changing microbial diversity and influent conditions (Reis et al., 2011).

Other parameters were also found to be significantly positively correlated with PHA composition including phosphorous availability in the SBR and nitrogen availability in the CSTR. Here, there are two potential reasons for why these are significantly correlated. First, it could be that these conditions are simply favorable for PHA storage and thus because the influent is P(3HB) dominated, it also favors higher P(3HB):P(3HV) ratio. Second, it could be that changing nutrient availability selects different microbial species which favor the conversion to one PHA species over another. Studies have shown different PHA composition within two reactors fed with the same influent, but different feeding regimes suggesting that nutrient availability and microbial diversity could be a determining factor (Reis et al., 2011).

4.3.4 Accumulation batch test: PHA composition

The claim of PHA composition changing with differently selected biomass is further supported by the batch testing which showed much higher P(3HV) content in the CSTR compared to the SBR for batch five and six which had the same 100% propionate influent feed. Batches done before solids removal had an opposite trend where the SBR had higher P(3HV) content than the CSTR (Bettex, 2021). Without microbial analysis, it cannot be established the true extent microbial dynamics play a role in PHA composition. However, there is indication that it may have an influence on the end PHAs measured. The tested condition of nitrogen availability in batch five and six did not have an influence on the PHA composition for the SBR (3.33 P(3HB):P(3HV)) ratio for both nitrogen limited and excess conditions). However, there was an effect observed for the CSTR: nitrogen limitation resulted in lower P(3HB):P(3HV) ratio of 0.3 as opposed to 0.4 with

nitrogen excess. This matches the positive correlation observed in the spearman correlation between nitrogen availability and P(3HB):P(3HV) ratio. Microbial diversity assessment would be a useful tool for clarifying why this pattern is observed.

5 Conclusion

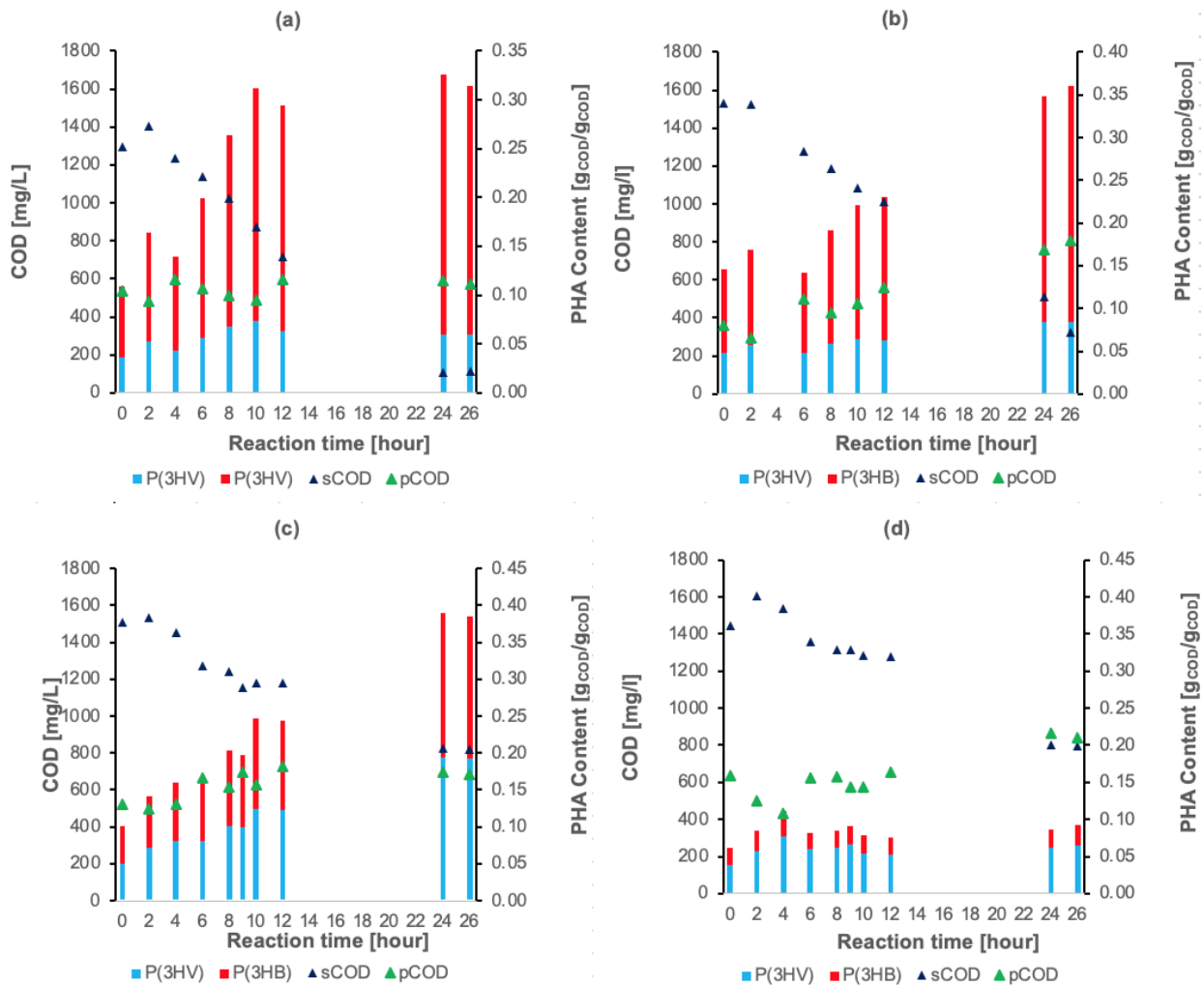
1. The removal of particulates from the influent allowed for more representative characterization of both systems.
2. Selection occurred and performed equally as well in the CSTR system when compared to the traditional SBR selection process before and after solids removal. Before solids removal, maximum PHA contents of 0.49 and 0.57 $\text{g}_{\text{COD}}/\text{g}_{\text{COD}}$ were found for the CSTR and SBR, respectively. After solids removal, maximum PHA contents of 0.25 and 0.36 $\text{g}_{\text{COD}}/\text{g}_{\text{COD}}$ were found for the CSTR and SBR, respectively.
3. The two reactor modes had different selection mechanisms that favored different PHA-storers. Before solids removal, the SBR selected biomass had higher PHA yield and contents than the CSTR selected biomass. After solids removal, the SBR selected biomass had higher PHA yield but lower contents than the CSTR selected biomass. For PHA composition, measurements showed higher P(3HB):P(3HV) in the CSTR biomass before solids removal but reversed after solids removal. Changing characterization of the selection and storage performance in the SBR and the CSTR selected biomass suggest that external factors such as influent nutrient availability and reactor environmental conditions may also govern the selection and storage mechanism. This was supported by multiple correlations found between influent nutrient availability and reactor environmental conditions and PHA content and composition. While correlations exist, causation cannot be confirmed in this study.
4. Accumulation tests showed that N-limitation governed PHA-storage in the CSTR with low relative PHA-storage increase of 182% under nitrogen excess and a high increase of 326% under N-limitation. For SBR systems, N-limitation had less of an effect, with relative increase of 312% under nitrogen limitation and relative increase of 247% under nitrogen excess, indicating that N-limitation does not play a primary role in inducing storage for the SBR selected PHA-storing biomass but does for the CSTR selected biomass. Future batch tests need to be completed without transient carbon feeding strategy to further clarify the contribution of N-limitation as a trigger for PHA storage.

References

- Albuquerque, M.G.E., Eiroa, M., Torres, C., Nunes, B.R., Reis, M.A.M., 2007. Strategies for the development of a side stream process for polyhydroxyalkanoate (PHA) production from sugar cane molasses. *J. Biotechnol.* 130, 411–421. <https://doi.org/10.1016/j.jbiotec.2007.05.011>
- Albuquerque, M.G.E., Torres, C.A.V., Reis, M.A.M., 2010. Polyhydroxyalkanoate (PHA) production by a mixed microbial culture using sugar molasses: Effect of the influent substrate concentration on culture selection. *Water Res.* 44, 3419–3433. <https://doi.org/10.1016/j.watres.2010.03.021>
- Beccari, M., Majone, M., Massanisso, P., Ramadori, R., 1998. A bulking sludge with high storage response selected under intermittent feeding. *Water Res.* 32, 3403–3413. [https://doi.org/10.1016/S0043-1354\(98\)00100-6](https://doi.org/10.1016/S0043-1354(98)00100-6)
- Bettex, C., 2021. Plastic is fantastic: Polyhydroxyalkanoate production on fermented wastewater sludge. *Eawag*.
- Braunegg, G., Lefebvre, G., Genser, K.F., 1998. Polyhydroxyalkanoates, biopolyesters from renewable resources: Physiological and engineering aspects. *J. Biotechnol.* 65, 127–161. [https://doi.org/10.1016/S0168-1656\(98\)00126-6](https://doi.org/10.1016/S0168-1656(98)00126-6)
- Cavaillé, L., Albuquerque, M., Grousseau, E., Lepeuple, A.S., Uribelarrea, J.L., Hernandez-Raquet, G., Paul, E., 2016. Understanding of polyhydroxybutyrate production under carbon and phosphorus-limited growth conditions in non-axenic continuous culture. *Bioresour. Technol.* 201, 65–73. <https://doi.org/10.1016/j.biortech.2015.11.003>
- Coats, E.R., Loge, F.J., Wolcott, M.P., Englund, K., McDonald, A.G., 2007. Synthesis of Polyhydroxyalkanoates in Municipal Wastewater Treatment. *Water Environ. Res.* 79, 2396–2403. <https://doi.org/10.2175/106143007x183907>
- Conca, V., da Ros, C., Valentino, F., Eusebi, A.L., Frison, N., Fatone, F., 2020. Long-term validation of polyhydroxyalkanoates production potential from the sidestream of municipal wastewater treatment plant at pilot scale. *Chem. Eng. J.* 390, 124627. <https://doi.org/10.1016/j.cej.2020.124627>
- Dionisi, D., Majone, M., Papa, V., Beccari, M., 2004. Biodegradable Polymers from Organic Acids by Using Activated Sludge Enriched by Aerobic Periodic Feeding. *Biotechnol. Bioeng.* 85, 569–579. <https://doi.org/10.1002/bit.10910>
- Estévez-Alonso, Á., Pei, R., van Loosdrecht, M.C.M., Kleerebezem, R., Werker, A., 2021. Scaling-up microbial community-based polyhydroxyalkanoate production: status and challenges. *Bioresour. Technol.* 327. <https://doi.org/10.1016/j.biortech.2021.124790>
- Johnson, K., Jiang, Y., Kleerebezem, R., Muyzer, G., Van Loosdrecht, M.C.M., 2009. Enrichment of a mixed bacterial culture with a high polyhydroxyalkanoate storage capacity. *Biomacromolecules* 10, 670–676. <https://doi.org/10.1021/bm8013796>
- Kleerebezem, R., Joosse, B., Rozendal, R., Van Loosdrecht, M.C.M., 2015. Anaerobic digestion without biogas? *Rev. Environ. Sci. Biotechnol.* 14, 787–801. <https://doi.org/10.1007/s11157-015-9374-6>
- Kourmentza, C., Plácido, J., Venetsaneas, N., Burniol-Figols, A., Varrone, C., Gavala, H.N., Reis, M.A.M., 2017. Recent advances and challenges towards sustainable polyhydroxyalkanoate (PHA) production. *Bioengineering* 4, 1–43. <https://doi.org/10.3390/bioengineering4020055>

- Ma, C.K., Chua, H., Yu, P.H.F., Hong, K., 2000. Optimal production of polyhydroxyalkanoates in activated sludge biomass. *Appl. Biochem. Biotechnol. - Part A Enzym. Eng. Biotechnol.* 84–86, 981–989. <https://doi.org/10.1385/abab:84-86:1-9:981>
- Michel, M., Jelmer, T., Ben, A., João, S., Henk, D., René, R., Robbert, K., 2020. Pilot-Scale Polyhydroxyalkanoate Production from Organic Waste: Process Characteristics at High pH and High Ammonium Concentration. *J. Environ. Eng.* 146, 4020049. [https://doi.org/10.1061/\(ASCE\)EE.1943-7870.0001719](https://doi.org/10.1061/(ASCE)EE.1943-7870.0001719)
- Ntaikou, I., Koumelis, I., Kamilari, M., Iatridi, Z., Tsitsilianis, C., Lyberatos, G., 2019. Effect of nitrogen limitation on polyhydroxyalkanoates production efficiency, properties and microbial dynamics using a soil-derived mixed continuous culture. *Int. J. Biobased Plast.* 1, 31–47. <https://doi.org/10.1080/24759651.2019.1648016>
- Oliveira-Filho, E.R., Silva, J.G.P., de Macedo, M.A., Taciro, M.K., Gomez, J.G.C., Silva, L.F., 2020. Investigating Nutrient Limitation Role on Improvement of Growth and Poly(3-Hydroxybutyrate) Accumulation by *Burkholderia sacchari* LMG 19450 From Xylose as the Sole Carbon Source. *Front. Bioeng. Biotechnol.* 7, 1–11. <https://doi.org/10.3389/fbioe.2019.00416>
- Puyol, D., Batstone, D.J., Hülsen, T., Astals, S., Peces, M., Krömer, J.O., 2017. Resource recovery from wastewater by biological technologies: Opportunities, challenges, and prospects. *Front. Microbiol.* 7, 1–23. <https://doi.org/10.3389/fmicb.2016.02106>
- Reis, M., Albuquerque, M., Villano, M., Majone, M., 2011. Mixed Culture Processes for Polyhydroxyalkanoate Production from Agro-Industrial Surplus/Wastes as Feedstocks, Second Ed. ed, *Comprehensive Biotechnology, Second Edition*. Elsevier B.V. <https://doi.org/10.1016/B978-0-08-088504-9.00464-5>
- Rhu, D.H., Lee, W.H., Kim, J.Y., Choi, E., 2003. Polyhydroxyalkanoate (PHA) production from waste. *Water Sci. Technol. a J. Int. Assoc. Water Pollut. Res.* 48, 221–228.
- Szacherska, K., Oleskiewicz-Popiel, P., Ciesielski, S., Mozejko-Ciesielska, J., 2021. Volatile fatty acids as carbon sources for polyhydroxyalkanoates production. *Polymers (Basel)*. 13, 1–21. <https://doi.org/10.3390/polym13030321>
- Thompson, D.N., Emerick, R.W., England, A.B., Flanders, J.P., Loge, F.J., Wiedeman, K.A., Wolcott, M.P., 2010. Final Report : Development of Renewable Microbial Polyesters for Cost Effective and Energy- Efficient Wood-Plastic Composites.
- Valentino, F., Moretto, G., Lorini, L., Bolzonella, D., Pavan, P., Majone, M., 2019. Pilot-Scale Polyhydroxyalkanoate Production from Combined Treatment of Organic Fraction of Municipal Solid Waste and Sewage Sludge. *Ind. Eng. Chem. Res.* 58, 12149–12158. <https://doi.org/10.1021/acs.iecr.9b01831>
- Valentino, F., Morgan-Sagastume, F., Campanari, S., Villano, M., Werker, A., Majone, M., 2017. Carbon recovery from wastewater through bioconversion into biodegradable polymers. *N. Biotechnol.* 37, 9–23. <https://doi.org/10.1016/j.nbt.2016.05.007>
- Vanwonterghem, I., Jensen, P.D., Rabaey, K., Tyson, G.W., 2015. Temperature and solids retention time control microbial population dynamics and volatile fatty acid production in replicated anaerobic digesters. *Sci. Rep.* 5, 1–8. <https://doi.org/10.1038/srep08496>
- Wen, Q., Chen, Z., Tian, T., Chen, W., 2010. Effects of phosphorus and nitrogen limitation on PHA production in activated sludge. *J. Environ. Sci.* 22, 1602–1607. [https://doi.org/10.1016/S1001-0742\(09\)60295-3](https://doi.org/10.1016/S1001-0742(09)60295-3)

Appendix



Appendix A: Batch 5a (a), 5b (b), 6a (c), and 6b (d) results showing PHA accumulation, consumption of sCOD and increase of pCOD over length of batch. Batches were stopped when sCOD consumption plateaued.